



Cite this: *Green Chem.*, 2024, **26**, 3595

## Photocatalyzed Minisci-type reactions for late-stage functionalization of pharmaceutically relevant compounds

Xiaotong Zhang,<sup>a</sup> Shuqi Li,<sup>a</sup> Feng Qiu,<sup>ID a,c</sup> Hwee Ting Ang,<sup>ID \*b</sup> Jie Wu<sup>ID \*b,d</sup> and Penghao Jia<sup>ID \*a</sup>

The Minisci-type reaction, as a versatile tool in the construction of substituted *N*-heteroarenes, has evolved rapidly since it was first realized and defined. The last decade has witnessed tremendous advances in Minisci-type reactions due to the advent of photoredox catalysis, reflected both in more abundant radical precursors and mild reaction conditions, which offers new opportunities for the functionalization of complex heteroarene-containing scaffolds. This review mainly focuses on the application of photocatalyzed Minisci-type reactions in the late-stage functionalization (LSF) of drugs and drug candidates, and it also includes mechanistic investigations concerning the generation of diverse radicals, aiming to accelerate the discovery of drug candidates and provide medicinal chemists with a comprehensive toolbox and guidance.

Received 22nd December 2023,  
Accepted 23rd February 2024

DOI: 10.1039/d3gc05089k

rsc.li/greenchem

### Introduction

The Minisci-type reaction, pioneered by Minisci in the 1960s,<sup>1–5</sup> involves the selective C–H functionalization of basic heteroarenes *via* a radical pathway. For over half a century,

these reactions have continuously evolved and now involve a wide range of radicals beyond conventional alkyl radicals, expanding their utility in C–H bond functionalization of heteroarenes.<sup>6–11</sup> While various Minisci-type reactions have been developed, their mechanism typically begins with the addition of a nucleophilic radical to a protonated electron-deficient heteroarene, forming radical intermediate **1** (Fig. 1). Subsequently, intermediate **1** can either lose its  $\alpha$ -proton through a direct hydrogen atom transfer (HAT) process and then undergo rearomatization (pathway 1) or undergo deprotonation and single electron transfer (SET) oxidation (pathway 2) to yield the protonated product.

*N*-heteroarenes are ubiquitous in pharmaceuticals, agrochemicals and natural products.<sup>12–14</sup> The structural analysis of

<sup>a</sup>School of Chinese Materia Medica, Tianjin University of Traditional Chinese Medicine, Tianjin 301617, China. E-mail: jiaph@tjutcm.edu.cn

<sup>b</sup>Department of Chemistry, National University of Singapore, Singapore 117543. E-mail: hweeting@nus.edu.sg, chmjie@nus.edu.sg

<sup>c</sup>Tianjin Key Laboratory of Therapeutic Substance of Traditional Chinese Medicine, Tianjin University of Traditional Chinese Medicine, Tianjin 301617, China

<sup>d</sup>National University of Singapore (Suzhou) Research Institute, Suzhou 215123, China



Xiaotong Zhang

Xiaotong Zhang received her BSc degree from Shenyang Pharmaceutical University in 2020. She has been pursuing her MSc degree under the supervision of Dr Penghao Jia in Tianjin University of Traditional Chinese Medicine. Her research interests are mainly focused on photoredox catalysis and medicinal chemistry.



Shuqi Li

Shuqi Li is an undergraduate student at the School of Chinese Materia Medica, Tianjin University of Traditional Chinese Medicine. She completed a college students' innovative entrepreneurial training plan program on photocatalytic modification of drugs under the supervision of Dr Penghao Jia in 2023.



carboxylation. Moreover, this approach has proven its effectiveness in LSF, as exemplified by the successful alkylation of fasudil, a potent vasodilator, at C1, to yield **1aa** in 50% yield within 16 hours under standard conditions.

In 2018, the Chen and Frenette groups independently reported a hypervalent iodine-mediated photo-alkylation of heteroarenes using benziiodoxole acetate (BI-OAc) and phenyliodine(III) bis(trifluoroacetate) (PIFA), respectively (Fig. 5).<sup>32,33</sup> Alkyl radicals were generated *via* reduction of an *in situ* formed iodonium ester (from carboxylic acid and hypervalent iodine reagent) by the excited photocatalyst followed by decarboxylation. Various biologically active molecules containing *N*-heteroarenes were successfully modified using these methods. For example, fasudil and quinoxifen were selectively alkylated, yielding **1ba** and **2a** with high efficiency. The versatility and robustness of these methods, even in the presence of amino and hydroxyl groups, was demonstrated by alkylating the antifungal voriconazole, the smoking-cessation drug varenicline, and the antimalarial quinine to yield **3a**, **4a** and **5aa**, respectively.

In 2020, Xu and Song disclosed an oxidant-free electrophotocatalytic Minisci alkylation using catalytic CeCl<sub>3</sub>·7H<sub>2</sub>O, representing a high atom-economy approach in the LSF of heteroarenes (Fig. 6).<sup>34</sup> The radical generation process begins with anodic oxidation of Ce(III) to Ce(IV), facilitating coordination with carboxylic acids, followed by a photoinduced ligand-to-metal charge transfer (LMCT) of the complex to generate Ce(III) and carboxyl radicals, which then undergo decarboxylation to yield the alkyl radicals. Various *N*-heteroarene containing drug molecules, such as fasudil, quinoxifen, voriconazole, and quinine, were well-tolerated to form **1ba**, **2a**, **3b** and **5ab** in

good to excellent yields. Moreover, pesticides diflufenican and chloantraniliprole as well as antihistamine drug loratadine were selectively alkylated at C-2 of pyridines to afford **6a**, **7a** and **8aa**. However, in the case of phosphodiesterase-3 inhibitor milrinone, a mixture of mono- and bis-alkylated products (**9a** and **9b**) was generated.

In 2018, Sherwood and co-workers developed an oxidant-free photoredox Minisci alkylation with carboxylic acids *via in situ*-generated *N*-(acyloxy)phthalimides (NAPs), where the alkyl radical was reductively generated from NAPs *via* the excited photocatalyst (Fig. 7).<sup>35</sup> This method exhibited tolerance towards various functional groups, as demonstrated by the successful alkylation of nucleosides and drug molecules, including quinine, camptothecin with a quinoline scaffold, nebularine, peracetylated nebularine, adenosine, and anti-cancer drug vemurafenib, with moderate to good yields. Despite the lower yield of adenosine (11%), which is likely due to the presence of an electron-donating amino substituent at C-6, this example highlighted the suitability of unprotected nucleosides with free hydroxyl and amines for this method. Additionally, alkylation of anticancer agent imatinib yielded a mixture of regioisomeric mono- and bis-alkylated products (**13a–13f**) in a combined yield of 48%.

With the advantages of not requiring external oxidants and ease of synthesis from carboxylic acids, NAPs have been widely employed in Minisci-type reactions.<sup>36–39</sup> In 2021, Zheng and co-workers reported a Minisci-type alkylation using NAPs in conjunction with diphenyl phosphate (PA) as the catalyst under metal- and photocatalyst-free conditions, where a photosensitive intermediate **I**, derived from PA and heteroarenes *via* hydrogen bonding, acts as a potent reducing agent to reduce



Jie Wu

Associate Prof. Wu Jie obtained his bachelor's degree in chemistry at Beijing Normal University in 2006. He then pursued his PhD study with Prof. James S. Panek at Boston University. In his postdoctoral research at MIT with Prof. Timothy Jamison and Prof. Alan Hatton, Jie was exposed to the significant aspects of continuous flow chemistry. Since joining NUS in July 2015, his research group focuses on synthetic meth-

odology development and on-demand synthesis of functionalized organic molecules assisted by flow technologies. In July 2021, Jie was promoted to tenured associate professor. Jie is a recipient of Dean's Chair Professor (2022), the Tokyo Chemical Industry-SNIC Industry Award in Synthetic Chemistry (2021), NUS Young Research Award (2021), Yong Scientist Award (2020), Asian Core Program Lectureship Award (2017–2022), and Thieme Chemistry Journal Award (2019).



Penghao Jia

Penghao Jia received her Ph.D. degree from Nankai University under the supervision of Prof. You Huang. She then joined the group of Prof. Jie Wu at the National University of Singapore for postdoctoral studies. In 2019, she started her independent career in Tianjin University of Traditional Chinese Medicine. Her principal research interest is in photoredox catalysis methodologies and biomolecule modifications.

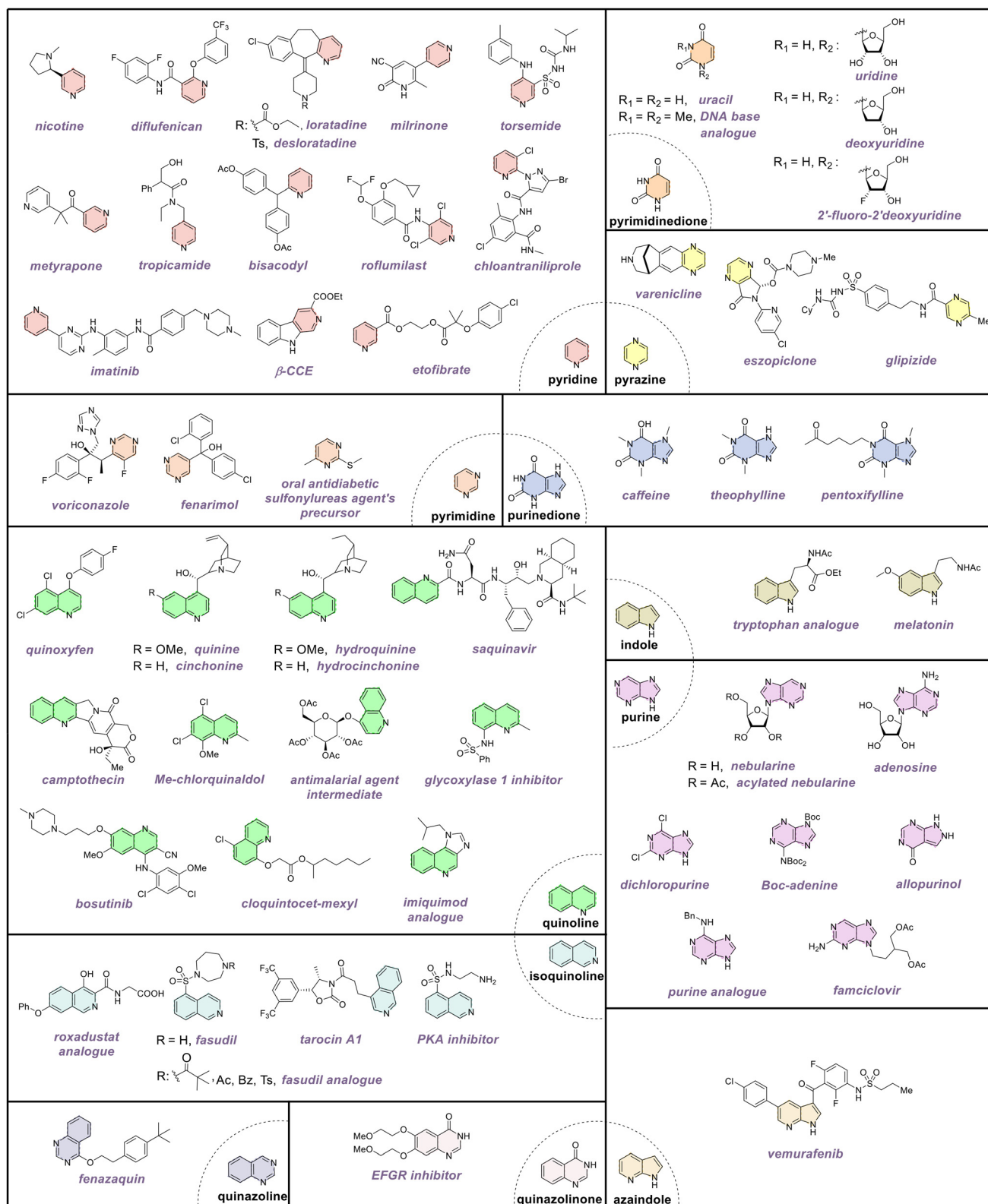


Fig. 2 List of pharmaceuticals that undergo LSF with Minisci-type reactions.



Fig. 3 Traditional Minisci alkylation reaction with carboxylic acids.

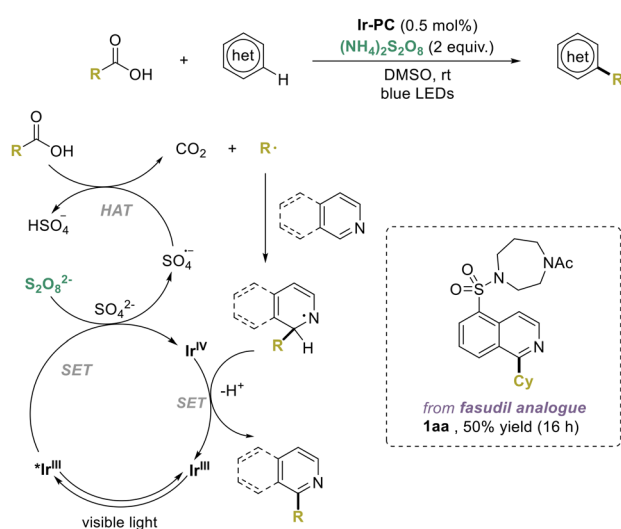


Fig. 4 Photoredox Minisci alkylation with carboxylic acids.

NAPs to form alkyl radicals (Fig. 8, condition 1).<sup>40</sup> This method was effectively applied to quinoxifen, producing **2b** in 54% yield. Similarly, Chan and co-workers introduced another approach facilitated by Hantzsch ester (HE), in which EDA complex **II**, formed *via* non-covalent interaction between HE and NAPs, plays a pivotal role in the generation of alkyl radicals under photoirradiation (Fig. 8, condition 2).<sup>41</sup> This approach yielded 68% yield of cyclohexylated quinine analogue **5ab**, outperforming the *in situ* generated NAPs in Sherwood's study.

### Organic peroxides as precursors

Besides carboxylic acids, organic peroxides can also serve as alkyl radical precursors. In 2014, DiRocco and co-workers reported photoredox catalyzed LSFs of biologically active

*N*-heteroarenes with small alkyl groups (*e.g.*, methyl, ethyl, and cyclopropyl) using stable organic peroxides (Fig. 9).<sup>42</sup> Complex molecules containing quinoline or isoquinoline moieties were selectively functionalized to generate **1bb**, **1bc**, **1bd**, **10b**, and **18a**. Furthermore, structures containing 6-membered heterocycles like pyrazines, pyrimidines, and pyridines reacted smoothly to yield methylated or cyclopropylated derivatives (**3c**, **3d**, **4b**, **4c**, **6b**, **8ab**, **14a**, **14b**, **15a**, **16a**, and **16b**). Even caffeine, which contains an imidazole unit (an electron-rich 5-membered heterocycle), was compatible with this method, yielding **17aa** with 52% yield. However, the use of such small alkyl radicals often leads to multiple alkylations.

### Alcohols and activated alcohols as precursors

Recent advances in photocatalysis have expanded the scope of alkyl radical precursors for Minisci alkylation to include abundant alcohols and activated alcohols. In 2015, MacMillan and co-workers utilized the synergistic merger of photoredox and thiol HAT organocatalysis, enabling primary alcohols to act as alkylating agents in Minisci-type reactions (Fig. 10).<sup>43</sup>  $\alpha$ -Oxy radicals are generated from alcohols *via* the HAT process with a thiyl radical (from the SET event between thiol and Ir(IV) species) and add to heteroarenes in the Minisci pathway. After deprotonation and spin-center shift (SCS), which forms benzylic radicals by eliminating a water molecule, the radicals are protonated and undergo a SET event with the excited photocatalyst, producing the alkylated product. The utility of this protocol in LSF was demonstrated by methylating fasudil with 82% yield using methanol and alkylation of milrinone with 3-phenylpropanol in 43% yield.

In 2019, Chen and co-workers also used alcohols as alkylating agents with hypervalent iodine BI-OAc as the oxidant under photoredox catalysis, compatible with primary, secondary, and tertiary alcohols (Fig. 11, condition 1).<sup>44</sup> Unlike MacMillan's work, alkyl radicals herein are generated *via*  $\beta$ -scission of alkoxy radical intermediates. Drug molecules like the fasudil derivative, quinine, and camptothecin were successfully alkylated with cyclohexylmethanol in good to high yields. In the same year, Liu and co-workers revealed another hypervalent iodine-mediated strategy using PIFA (Fig. 11, condition 2), allowing the LSF of a plethora of natural products and drug molecules with alcohols.<sup>45</sup> The fasudil derivative, quinoxifen, quinine, and fenazaquin (a quinazoline-based insecticide) reacted smoothly yielding **1cb**, **2d**, **5ac**, and **19a** in good yields. However, the famciclovir derivative resulted in a mixture of monoalkylated and dialkylated products (**17ba** and **17bb**). More recently, in 2022, Zhu and Li developed a similar reaction in stop-flow microtubing (SFMT) reactors, where quinoxifen and voriconazole were functionalized with 2-methylpropan-1-ol to give **2c** and **3a** in moderate yields (Fig. 11, condition 3).<sup>46</sup>

In 2019, Overman and co-workers described the use of *tert*-alkyl oxalates (activated alcohols derived from tertiary alcohols) as alkylating agents under photocatalytic conditions (Fig. 12, condition 1).<sup>47</sup> Later in the same year, Wang and co-workers also employed alkyl oxalates derived from primary,

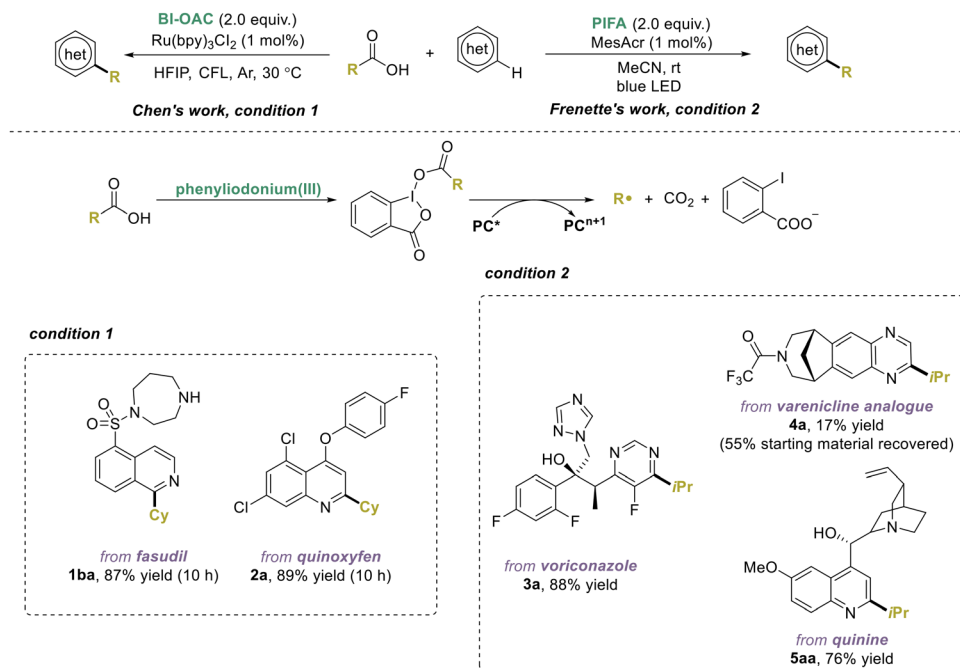


Fig. 5 Hypervalent iodine-promoted Minisci alkylations.

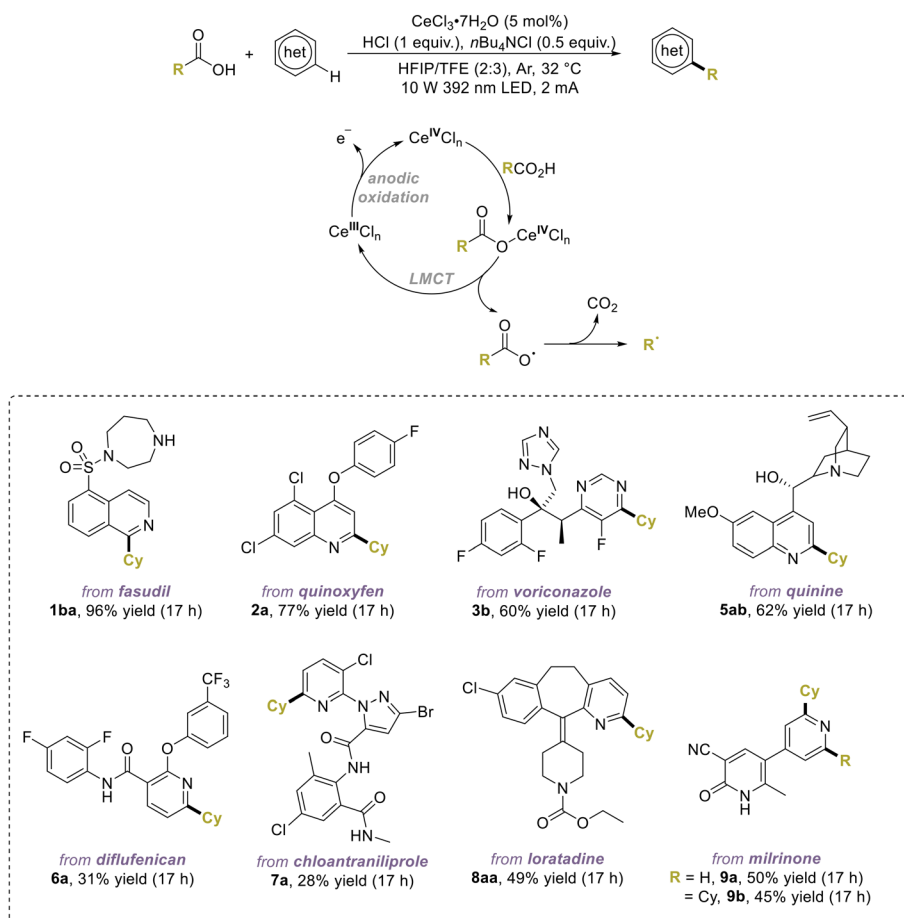


Fig. 6 Electrophotocatalytic Minisci alkylation of heteroarenes with carboxylic acids.



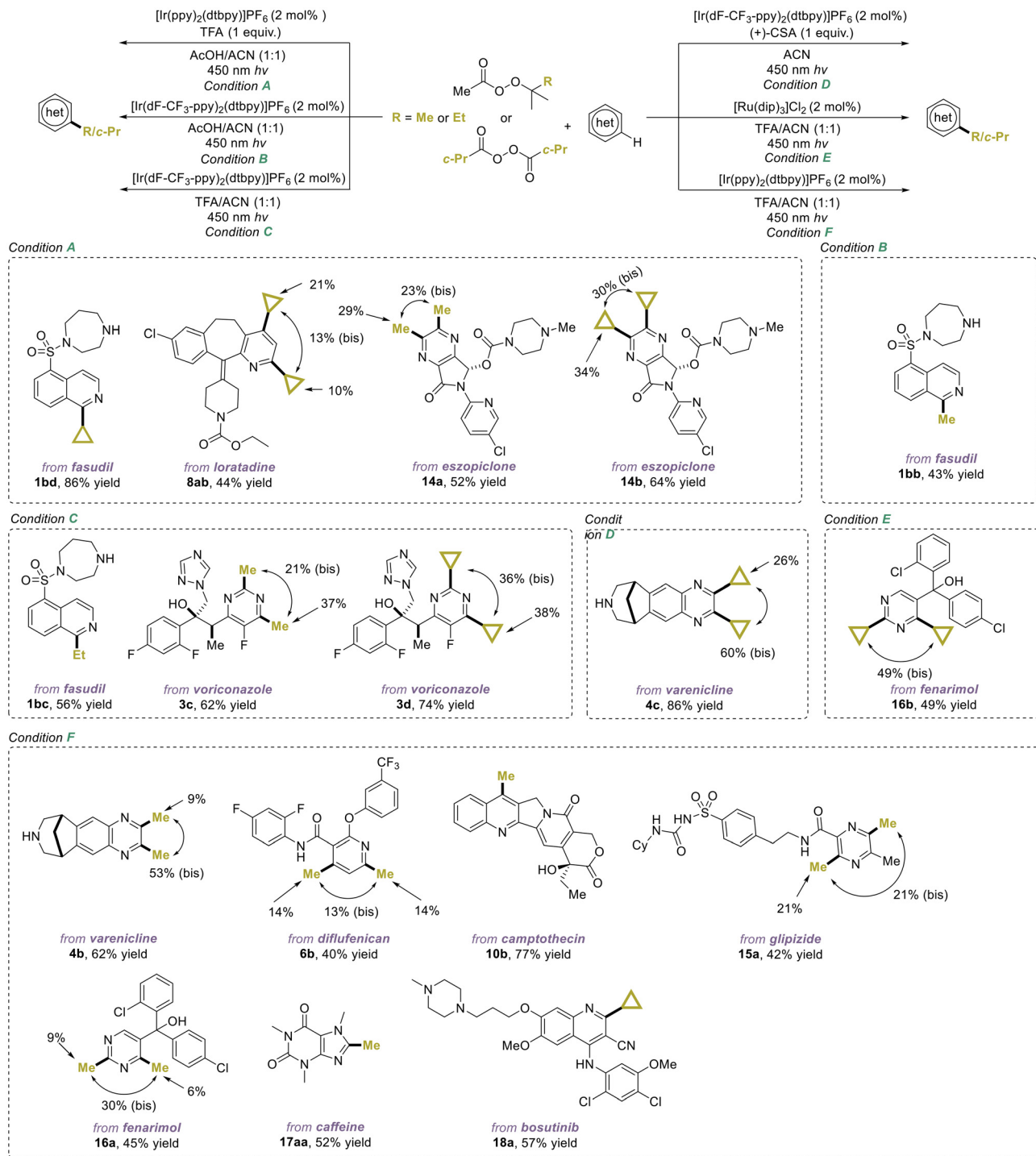


Fig. 9 Photoredox Minisci alkylation using organic peroxides.

and co-workers developed a photocatalytic strategy to generate  $\alpha$ -oxy radicals from these compounds through reductive proton-coupled electron transfer (PCET) with a strongly reducing Ir(III) species, generated from the excited photocatalyst and tris(trimethylsilyl)silane (TTMSS) (Fig. 13, condition 1).<sup>49</sup> The  $\alpha$ -oxy radicals subsequently add to heteroarenes *via* a Minisci-type pathway, and the final product is formed from

benzylic radicals through a series of SCS and HAT processes. Natural products and drug molecules, such as loratadine, milrinone, etofibrate, and the steroidogenesis inhibitor metyrapone, were successfully alkylated with various ketones in moderate yields. Later, Huang and co-workers also reported a photocatalysis protocol in which both aliphatic and aromatic aldehydes were effective alkylating reagents (Fig. 13, condition

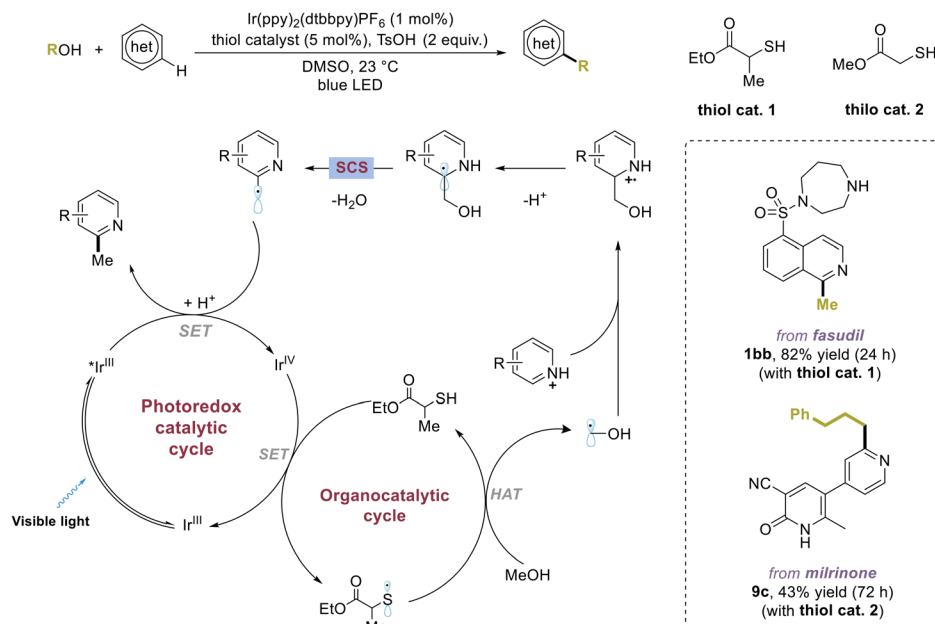


Fig. 10 Photoredox Minisci alkylations with alcohols via a SCS process.

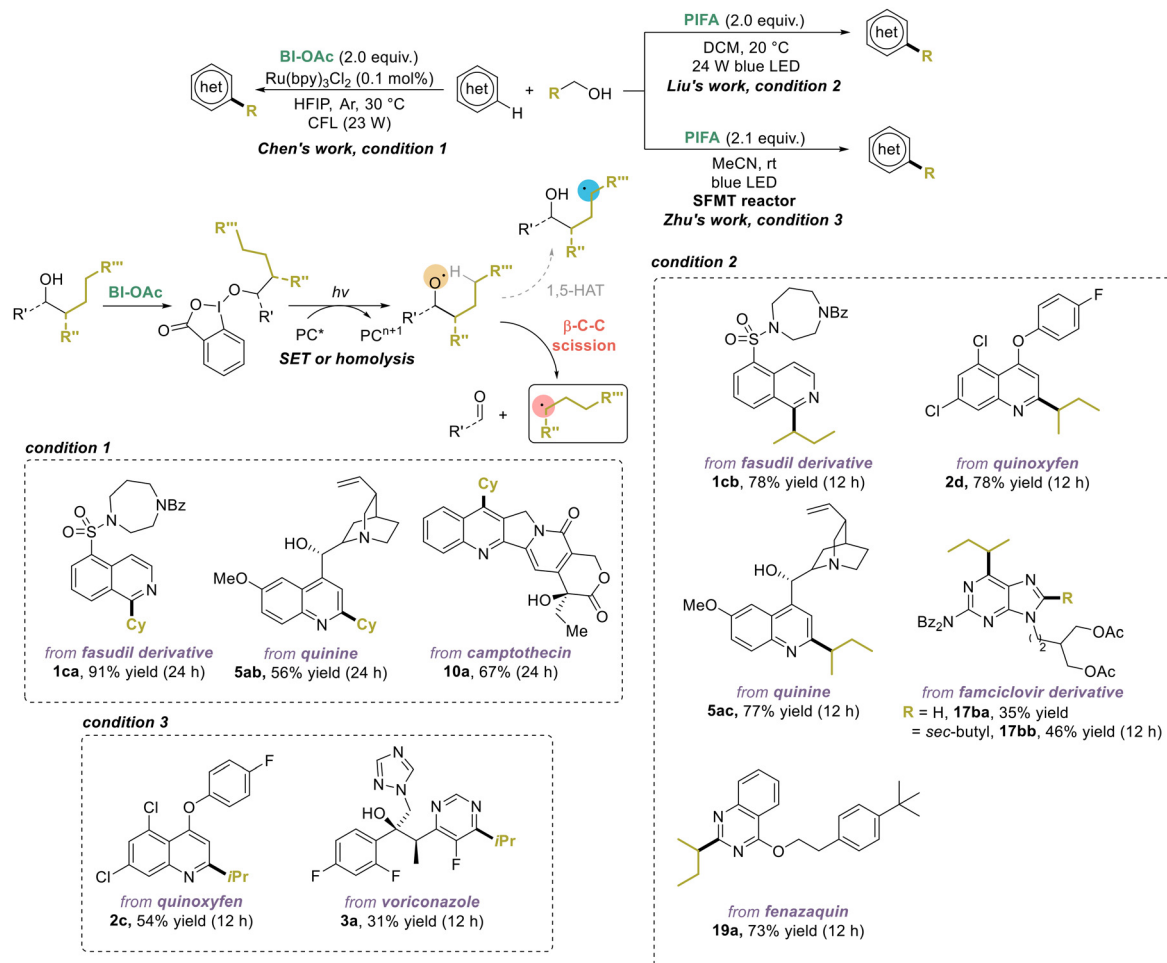


Fig. 11 Photoredox Minisci alkylations with alcohols via  $\beta$ -scission of alkoxy radical intermediates.

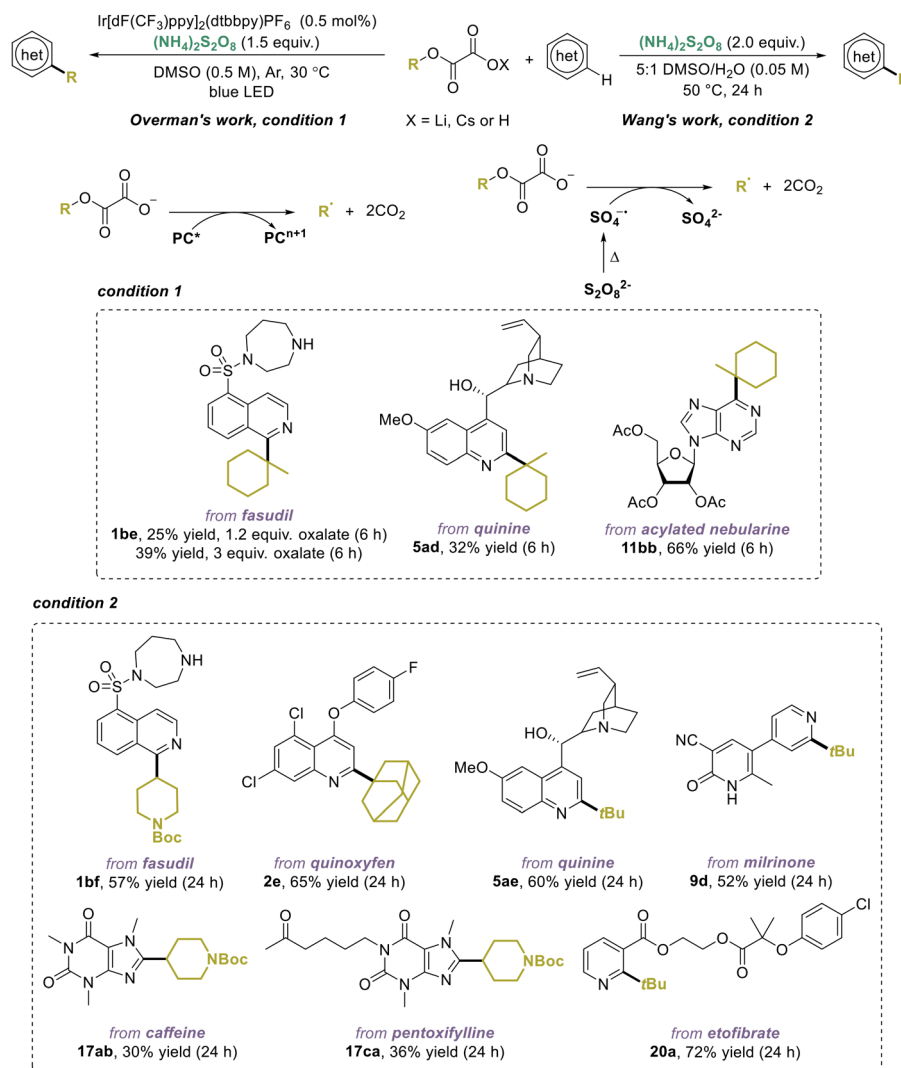


Fig. 12 Minisci alkylations with oxalates as alkylating agents.

2).<sup>50</sup> Using slightly modified reaction conditions, biologically active molecules were functionalized with isobutyraldehyde or benzaldehyde with moderate to good yields (**1cc**, **2f**, **2g**, and **5ba**).

In 2019, Huang and co-workers developed an alternative approach under ambient air conditions, where alkyl radicals are generated from aldehydes through a HAT process (Fig. 14, condition 1).<sup>51</sup> In 2022, Zhu and co-workers also revealed a similar approach in the presence of PIFA (Fig. 14, condition 2).<sup>52</sup> Notably, quinoxifen, quinine, and voriconazole were alkylated with aliphatic aldehydes in good to excellent yields. Noteworthy, these reactions can be operated in open air without the need for inert gas protection, making them particularly suitable for the LSF of pharmaceutically relevant compounds.

In 2017, Molander and co-workers presented an indirect utilization of aldehydes as alkyl radical precursors by employing 1,4-dihydropyridines (DHPs) as masked aldehydes and per-

sulfate as the oxidant without light irradiation.<sup>53</sup> Building on this, in 2020, Wang and co-workers demonstrated photocatalytic Minisci alkylation with DHPs using  $\text{O}_2$  as a green oxidant (Fig. 15).<sup>54</sup> In this strategy, DHPs are oxidized by the photoexcited  $^*\text{Ir}(\text{III})$  complex to generate alkyl radicals and substituted pyridines. Various complex molecules were functionalized using this method, yielding the corresponding products in moderate to good yields (**1bg**, **2c**, **5bb**, **9f**, and **20a**).

### Organoboron as a precursor

In the past decade, organoboron compounds have also emerged as versatile radical precursors for Minisci-type alkylation. In 2010, Baran and co-workers first showed the use of arylboronic acids for Minisci alkylation using  $\text{Ag}(\text{I})/\text{S}_2\text{O}_8^{2-}$  as an oxidant.<sup>55</sup> Later, in 2016, Chen and co-workers developed a photoredox alternative for primary and secondary alkylboronic



Fig. 13 Photoredox Minisci alkylations with carbonyls via PCET and SCS mechanism.



Fig. 14 Photoredox Minisci alkylations with carbonyls via HAT and decarbonylation.

acids using BI-OAc as an oxidant (Fig. 16, condition 1).<sup>56</sup> The *ortho*-iodobenzoyloxy radical, generated from BI-OAc via a SET process with the excited photocatalyst, reacts with alkylboronic acids to generate alkyl radicals for the Minisci-type reaction.

Various natural products and drug molecules with diverse functional groups were alkylated with alkylboronic acids in moderate to good yields (**1bc**, **5ab**, **5af**, **10a**, **10c**, **16c–16e**, **17ac**, **17ad**, and **17bc–17bf**). Notably, famciclovir, a guanine ana-

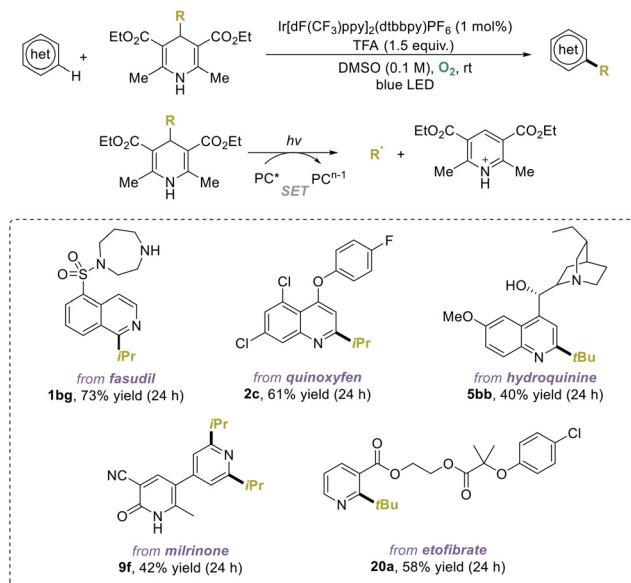


Fig. 15 Photoredox Minisci alkylations with DHPs.

logue antiviral drug, could be functionalized with alkyl chains bearing an alkynyl or alkyl bromide group in good yields. In 2020, Wang and co-workers reported another strategy using molecular  $O_2$  as a clean oxidant, particularly suitable for the LSF of complex molecules (Fig. 16, condition 2, **1ba**, **2a**, **8aa**, **10a**, **17da**, and **20d**).<sup>57</sup>

Trifluoroborates can also be employed in Minisci-type reactions, first introduced by Molander and colleagues in 2011 by using excess  $Mn(OAc)_3$  as the oxidant.<sup>58</sup> In 2017, they refined the method, enabling the use of primary, secondary, and tertiary alkyltrifluoroborates as alkyl radical precursors under mild photoredox conditions (Fig. 17, condition 1).<sup>59</sup> Here, trifluoroborates undergo single-electron oxidation to generate alkyl radicals in the presence of catalytic amounts of Fukuzumi's organophotocatalyst (MesAcr) and stoichiometric persulfate at room temperature. In 2019, Xu and co-workers reported another approach by merging electro- and photoredox catalysis, enabling an oxidant-free approach for alkyl radical generation from trifluoroborates (Fig. 17, condition 2).<sup>60</sup> Various alkyltrifluoroborates were successfully applied in the LSF of bioactive compounds under these conditions, with Molander's strategy with persulfates giving higher yields than the photoelectrochemical conditions.

In 2021, Li and co-workers reported a synergistic merger of a novel quinoline-based organophotoredox catalyst, namely 2,4-bis(4-methoxyphenyl)quinoline (DPQN<sup>2,4-di-OMe</sup>), and chloro(pyridine)cobaloxime catalyst for the oxidant-free generation of alkyl radicals from trifluoroborates (Fig. 18).<sup>61</sup> The alkylation of substrates with high molecular complexity was explored, yielding the desired products, such as **1ba**, **3b**, **5ca**, **8aa**, **17eb**, **22a**, and **23a**, in moderate to good yields.

## Alkyl halides as precursors

Alkyl halides can serve as alkyl radical precursors through halogen atom abstraction (XAT) in Minisci alkylation. In 2017, Fadeyi and co-workers employed  $Mn_2(CO)_{10}$  as a catalyst to generate alkyl radicals from alkyl iodides under photoirradiation, where the Mn–Mn bond in  $Mn_2(CO)_{10}$  undergoes photochemical homolytic cleavage and facilitated the subsequent iodine atom abstraction (Fig. 19).<sup>62</sup> The utility of this protocol was demonstrated by the LSF of the highly functionalized peptidic drug saguinavir with iodocyclopentane and iodoisopropane, as well as the biotinylation of bosutinib with iodobiotin, albeit in a low yield.

In 2019, Wang and co-workers utilized alkyl bromides as alkyl radical sources under photocatalytic conditions, with tris(trimethylsilyl) silane (TTMSS) as the XAT agent and molecular  $O_2$  as the oxidant (Fig. 20, condition 1).<sup>63</sup> In the same year, ElMarrouni and co-workers reported a similar protocol by using persulfate as the oxidant instead (Fig. 20, condition 2).<sup>64</sup> It was proposed that a bromine radical, formed through the oxidation of  $Br^-$  by the photocatalyst, undergoes HAT with TTMSS to provide silyl radical species, which then abstract a bromine atom from alkyl bromides, forming alkyl radicals. The LSF of drug molecules containing *N*-heteroarenes proceeded smoothly, affording the alkylated products in moderate to good yields, with ElMarrouni's protocol requiring shorter reaction times (4 h vs. 24 h).

## Alkanes as precursors

Direct utilization of alkanes as alkyl radical sources represents the most straightforward and atom-economical approach in Minisci alkylations. Numerous HAT reagents have been applied to generate alkyl radicals *via*  $C(sp^3)-H$  abstraction.<sup>65</sup> In 2019, Li and co-workers employed diacetyl (2,3-butanedione) as the energy transfer (ET) reagent and di-*tert*-butyl peroxide (DTBP) as the HAT reagent to generate alkyl radicals from otherwise unactivated alkanes (Fig. 21).<sup>66</sup> Promisingly, valuable substrates including quinine and nicotine were effectively functionalized using cyclohexane.

In 2019, both the Lei and Jin groups independently reported a photocatalyst-free strategy using Selectfluor as both the HAT reagent and oxidant (Fig. 22, condition 1).<sup>67,68</sup> Under photoirradiation, Selectfluor undergoes N–F homolytic cleavage to give *N*-radical cation intermediate **III**, which serves as a HAT reagent to deliver alkyl radicals from unactivated alkanes. In the same year, Jin and co-workers also utilized  $H_2O_2$  as both the HAT reagent and oxidant (Fig. 22, condition 2).<sup>69</sup> Similarly, upon photoirradiation, hydroxyl radical **IV** is formed *via* homolytic O–O bond cleavage and serves as the HAT reagent. Notably, complex molecules including fasudil, quinoxifen, voriconazole, and roflumilast readily underwent alkylation under these two photocatalyst-free protocols.

Due to the relatively large bond dissociation energies (BDE) of HCl ( $102 \text{ kcal mol}^{-1}$ ),<sup>70</sup> the use of the chlorine radical ( $Cl^\bullet$ ) as the HAT reagent for unactivated alkanes in Minisci reac-



Fig. 16 Photoredox Minisci-type alkylations with alkylboronic acids.

tions has been explored. In 2020, Xu and co-workers reported an oxidant-free approach by merging electrochemistry and photochemistry, where  $\text{Cl}^\cdot$  is generated by the anodic oxidation of  $\text{Cl}^-$  followed by the light-promoted homolytic cleavage of the resultant  $\text{Cl}_2$  (Fig. 23).<sup>71</sup> This photoelectrochemical method was successfully applied to alkylate purine derivatives and bioactive compounds. In 2021, Li and co-workers developed another oxidant-free protocol using catalytic *tert*-butylammonium chloride and a cobaloxime catalyst under photoirradiation (Fig. 24).<sup>72</sup> Acetylated fasudil, caffeine, purine, and nicotine were alkylated with moderate yields. Hydrocinchonine, a commonly used chiral ligand in synthetic chemistry, underwent alkylation while preserving its hydroxy group. Also in 2021, Liu and Zhang disclosed another protocol under an aerobic atmosphere with cerium chloride as the photocatalyst

and air as the oxidant, enabling the alkylation of quinoxifen and theophylline in moderate yields (Fig. 25).<sup>73</sup>

In 2020, Li and An reported a photo-induced ET approach using 4-CzIPN as the catalyst, where ET occurs from the photoexcited 4-CzIPN\* to  $(\text{NH}_4)_2\text{S}_2\text{O}_8$ , resulting in the homolysis of peroxydisulfate into the sulfate radical anion that serves as the HAT reagent (Fig. 26).<sup>74</sup> The robustness of this protocol was demonstrated by the LSF of complex molecules, such as fasudil, hydroquinone, and cinchonine, affording the alkylated products in moderate yields.

In 2022, Deng and Wu introduced an oxidant-free, SFMT reactor-assisted approach, in which the HAT reagent, diphenylphosphate radical, was generated from diphenylphosphate anion *via* SET with the photoexcited acridinium photocatalyst (Fig. 27).<sup>75</sup> Various complex bioactive molecules underwent

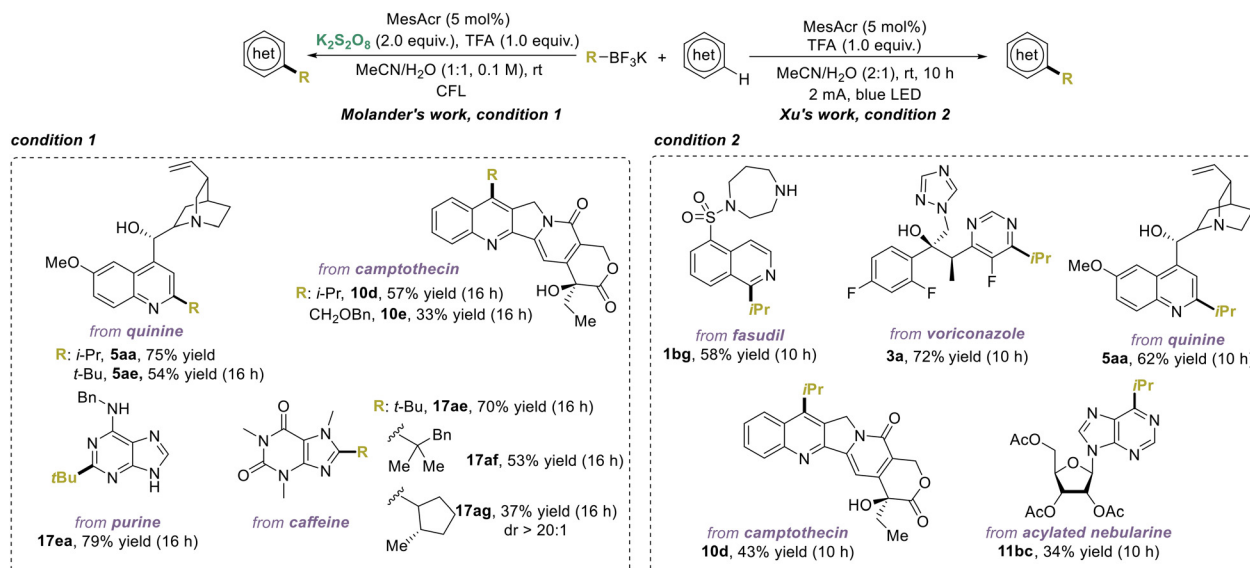


Fig. 17 Photoredox Minisci alkylations with trifluoroborates.

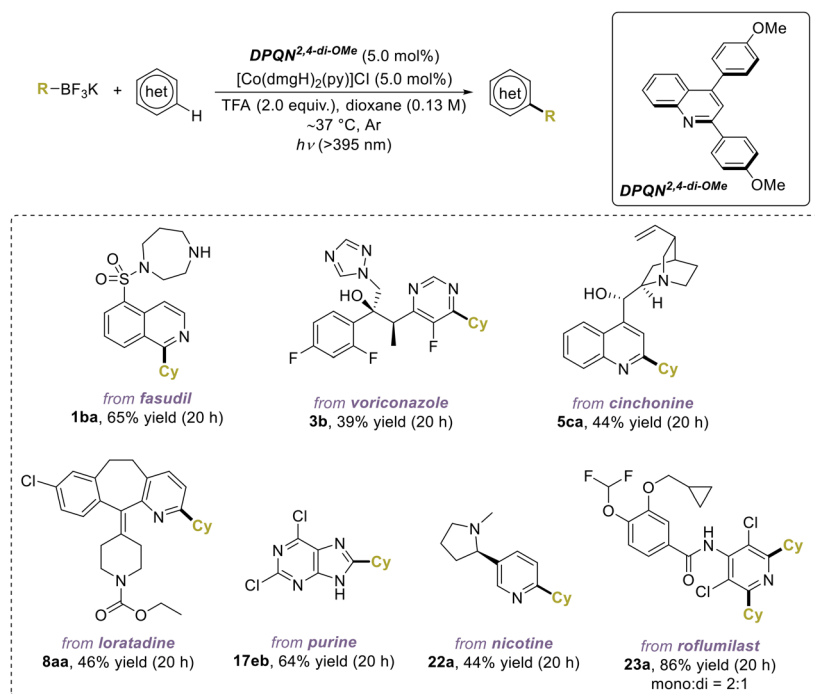


Fig. 18 A quinolinium/cobaloxime dual photocatalytic system for Minisci alkylations with trifluoroborates.

the LSF smoothly, highlighting the effectiveness of this approach.

## Introduction of ethers, alcohols, amines, and amides

Moving beyond the introduction of alkyl groups, the range of Minisci reactions has extended to incorporate diverse func-

tional groups, such as ethers, alcohols, amines, and amides, in *N*-heteroarenes.

### Ethers, alcohols, amines, and amides as precursors

In 2015, MacMillan and co-workers pioneered a photoredox Minisci reaction with ethers, both cyclic and acyclic, using Ir [dF(CF<sub>3</sub>)ppy]<sub>2</sub>(dtbbpy)PF<sub>6</sub> as the photoredox catalyst and Na<sub>2</sub>S<sub>2</sub>O<sub>8</sub> as the oxidant (Fig. 28).<sup>76</sup> The α-oxyalkyl radicals are produced from ether through a HAT process with the sulfate

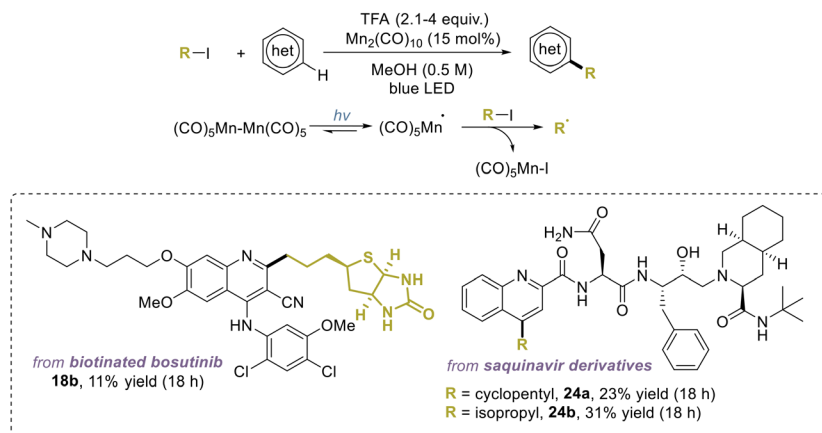


Fig. 19 Photocatalyzed Minisci alkylations with alkyl iodides.

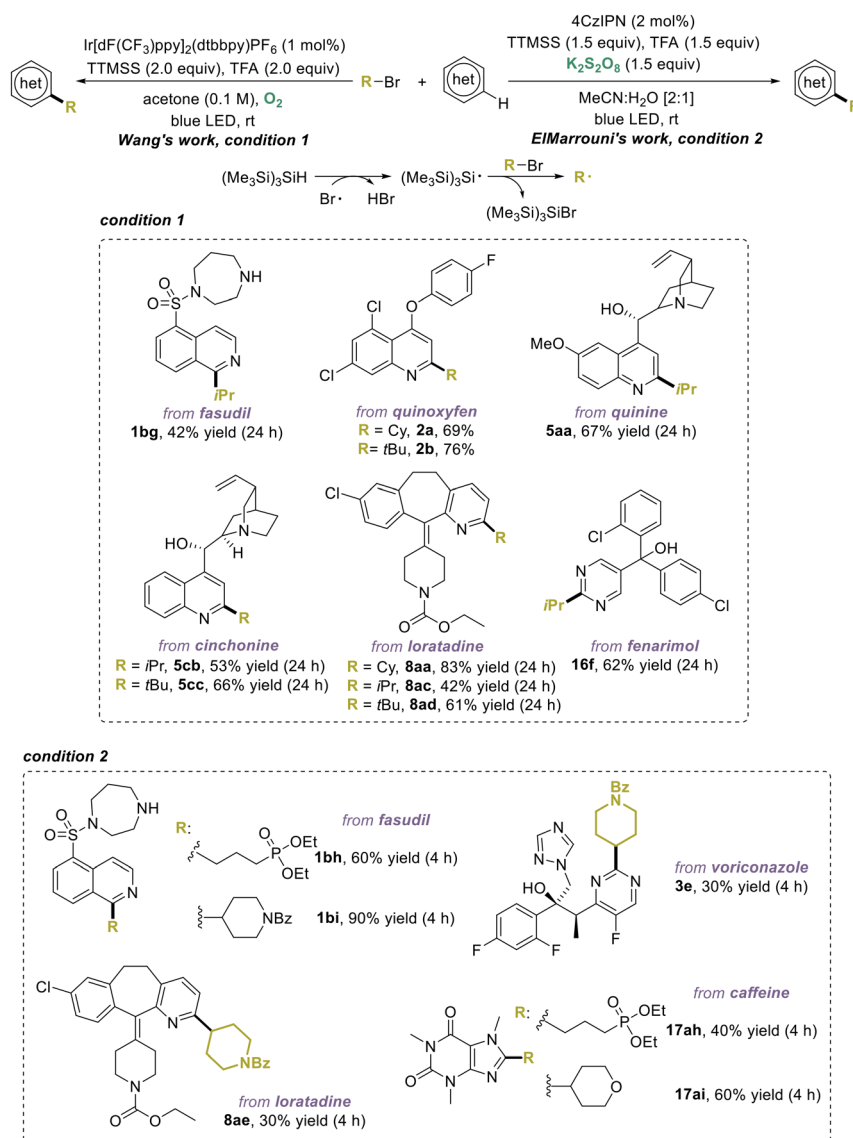


Fig. 20 Photocatalyzed Minisci alkylations with alkyl bromides.



**Fig. 21** Minisci alkylations of alkanes with diacetyl as the photosensitizer.

radical anion, produced by the SET process between  $\text{Na}_2\text{S}_2\text{O}_8$  and the photo-excited photocatalyst.

Using a similar strategy, in 2018 and 2019 respectively, Wang and Johnson research groups independently reported the use of amines as radical precursors to introduce an *N*-protected amine functionality (Fig. 29).<sup>77,78</sup> The  $\alpha$ -aminoalkyl radicals are generated from amine through HAT with *tert*-butoxy radical (Fig. 29, condition 1) or sulfate radical anion (Fig. 29, condition 2). This strategy enabled the selective aminoalkylation of pentoxifylline at C2 with 52% yield, and fasudil was also successfully functionalized using both methods in moderate yields.

In 2019, another approach for the Minisci oxyalkylation was reported by Li and co-workers, using diacetyl as both a triplet-state photosensitizer and HAT reagent to generate the alkyl radicals from ethers (Fig. 30).<sup>66</sup> Moderate to good yields were

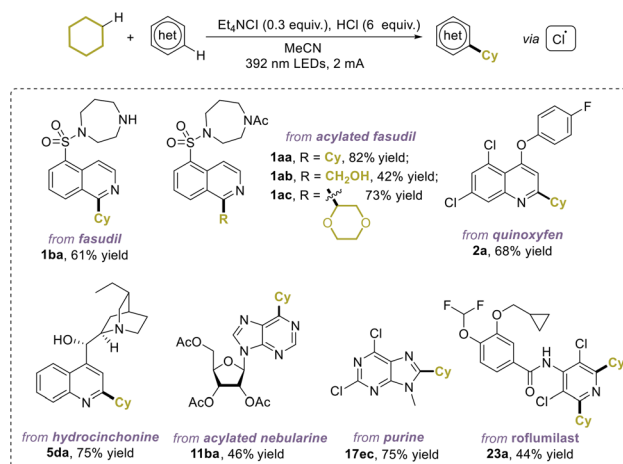


**Fig. 23** Photoelectrochemical Minisci alkylations with alkanes via  $\text{Cl}^\bullet$ .

obtained in the functionalization of complex molecules under this approach.

In 2021, Guin and co-workers developed a general protocol under air that can incorporate both oxygen and nitrogen functionalities (ethers, amides, and alcohols) in *N*-heteroarenes (Fig. 31).<sup>79</sup> It utilizes singlet oxygen, generated *in situ* upon irradiation of air with a 370 nm LED lamp, as the HAT reagent. The robustness of the method was demonstrated by the LSF of biologically relevant natural products with ethers and amides.

In 2016, DiRocco and Krska disclosed a photoredox Minisci hydroxymethylation with methanol using an iridium photocatalyst and benzoyl peroxide (BPO) as the HAT reagent precursor, which generates the HAT reagent (phenyl radical) from BPO *via* SET with the photoexcited  $^*\text{Ir(III)}$  complex and decomposition (Fig. 32).<sup>80</sup> With this method, the hydroxymethylation of fasudil and torsemide, a loop diuretic, afforded **1bl** and **27a** as a single regioisomer, while modification of voriconazole, with a pyrimidine core, resulted in a mixture of regioisomers.



**Fig. 22** Photocatalyst-free Minisci alkylations with alkanes.



Fig. 24 Photoinduced Minisci alkylations with alkanes using catalytic chloride and cobalt catalyst.

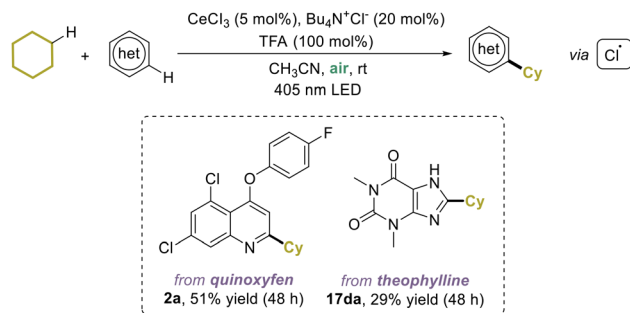


Fig. 25 Photocatalyzed Minisci alkylations using alkanes under an aerobic atmosphere.



Fig. 26 Minisci alkylations with alkanes via an ET process.

Another strategy based on the regioselective 1,5-HAT process has also been developed to introduce distal alcohol or amide functionalities to *N*-heteroarenes via the Minisci reaction. In 2018, Zhu and co-workers introduced a metal-free approach using PIFA as the sole reagent in DCM (Fig. 33, condition 1).<sup>81</sup> They later reported a greener variant in 2022, using



Fig. 27 Photocatalyzed Minisci alkylations with alkanes assisted by SFMT reactors.

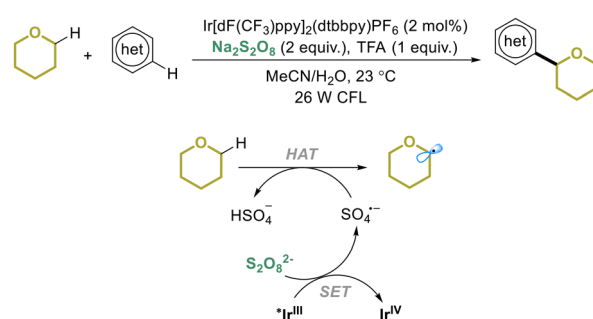


Fig. 28 Photoredox Minisci reactions with ethers.

MeCN as the solvent and SFMT reactor (Fig. 33, condition 2).<sup>82</sup> In 2019, Chen and co-workers employed perfluorinated hydroxybenziodoxole (PFBI-OH) as the oxidant for this strategy (Fig. 33, condition 3).<sup>83</sup> This strategy generally involves the generation of alkoxy radicals from free alcohols under photoirradiation and subsequent 1,5-HAT reactions that furnish carbon-centered radicals for Minisci reactions. This approach efficiently coupled alcohols with complex drug molecules, yielding the desired products. Notably, taracin A1, an inhibitor of TarO enzyme, reacted with 1-butanol to yield **28a** bearing a distal alkyl alcohol handle in 78% yield.

In 2019, Yu and co-workers expanded this strategy to introduce a distal amide group on *N*-heteroarenes, using hydroxamide as a precursor (Fig. 34, condition 1).<sup>84</sup> The amidyl radical, derived from hydroxamide through SET with the photo-excited photocatalyst, undergoes a 1,5-HAT process to yield alkyl radicals for the Minisci reaction. Famciclovir was successfully modified to give **17bh** in a 51% yield with this protocol. Also in 2019, Chen and colleagues developed another

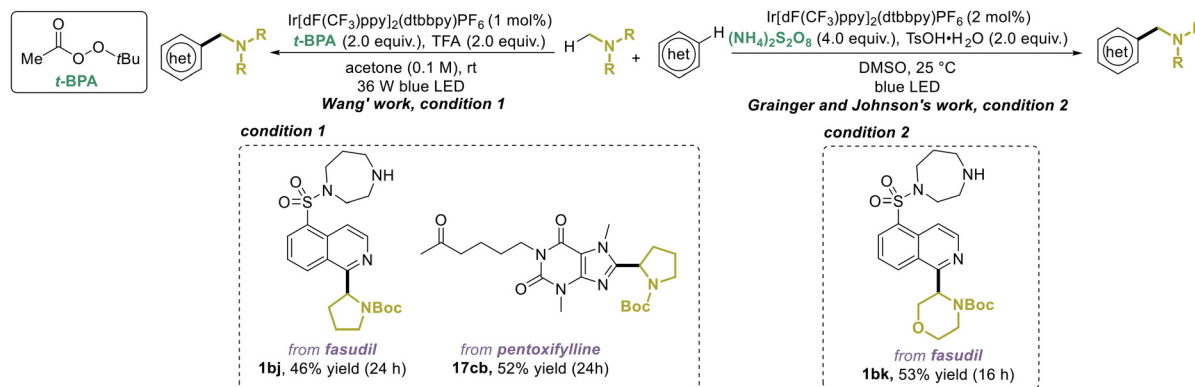


Fig. 29 Photoredox Minisci aminoalkylation with amines.

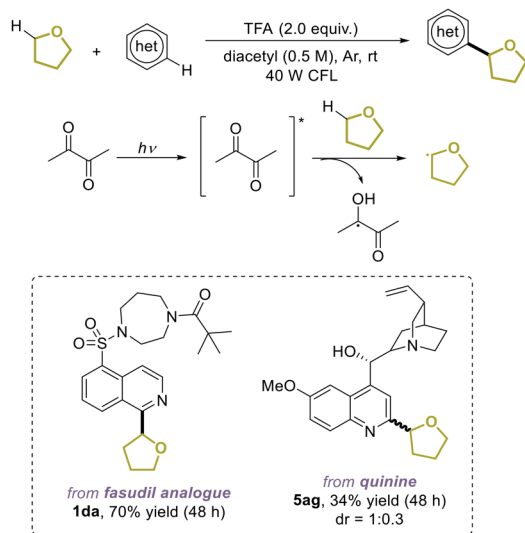


Fig. 30 Minisci oxyalkylations using diacetyl as the photosensitizer and HAT reagent.

protocol using sulfonyl-protected primary aliphatic amines (Fig. 34, condition 2), enabling the efficient introduction of a distal sulfonyl-protected amine to *N*-heteroarenes, such as fasudil derivatives.<sup>85</sup>

### Amino acid derivatives as precursors

Amino acids have been used to introduce  $\alpha$ -amine moieties to *N*-heteroarenes *via* Minisci-type reactions by leveraging the well-established generation of alkyl radicals from carboxylic acids. In 2017, using a combination of photoredox and Brønsted acid catalysis, Fu and Shang reported an  $\alpha$ -aminoalkylation of complex *N*-heteroarenes, such as fasudil, caffeine, and famciclovir, with amino acid-derived NAPs (Fig. 35, condition 1).<sup>86</sup> In 2018, Phipps and co-workers demonstrated an enantioselective variant of this transformation using an enantiopure chiral Brønsted acid catalyst (*R*)-TCYP for the asymmetric induction (Fig. 35, condition 2).<sup>87</sup> This method enabled excellent regio- and enantioselective

functionalization of etofibrate and metyropone (**20e**, 93% ee; **21b**, 95% ee).

In 2019, Wang and co-workers described another strategy using easily reduced *N*-hydroxybenzimidoyl chloride (NHBC) esters as the radical precursor under photoredox conditions without the need for a Brønsted acid catalyst (Fig. 36).<sup>88</sup> This protocol was effective in modifying etofibrate, yielding **20f** with 75% yield.

### Aldehydes as precursors

In 2020, the use of aldehydes as a precursor for Minisci  $\alpha$ -hydroxyalkylation was reported by Kanai and Mitsunuma, using an acridinium photocatalyst and a thiophosphoric acid (TPA) organocatalyst (Fig. 37).<sup>89</sup> Mechanistic studies indicated that the thiyl radical (generated from TPA *via* SET with the excited photocatalyst) initiates a HAT process with aldehydes to produce acyl radicals, which then undergo Minisci reactions, yielding the final products after a sequence of deprotonation, SCS, SET, and protonation processes. Notably, the reaction conditions enabled efficient  $\alpha$ -hydroxyalkylation of a fasudil derivative and camptothecin within 3 hours.

In 2019, Melchiorre and co-workers described a photocatalyst- and oxidant-free  $\alpha$ -hydroxyalkylation by using 4-acyl-1,4-dihydropyridines (acyl-DHPs), which can be prepared in one-step from alkyl- and aryl-glyoxals, as acyl radical precursors (Fig. 38).<sup>90</sup> Upon photoirradiation, acyl-DHPs generated acyl radicals through facile SET reduction and homolytic cleavage. This approach efficiently functionalized complex molecules with quinoline cores, demonstrating its synthetic potential with moderate to good yields.

## Introduction of aryl groups

Aryl-heteroaryl skeletons, known for their significant biological and medicinal properties,<sup>91</sup> can also be constructed through photocatalyzed Minisci reactions. In 2014, Xue and co-workers generated aryl radicals from aryldiazonium salts through SET reduction by the photo-excited  $^*Ru(II)$  complex and extrusion of  $N_2$  in aqueous formic acid (Fig. 39).<sup>92</sup> Using this method,

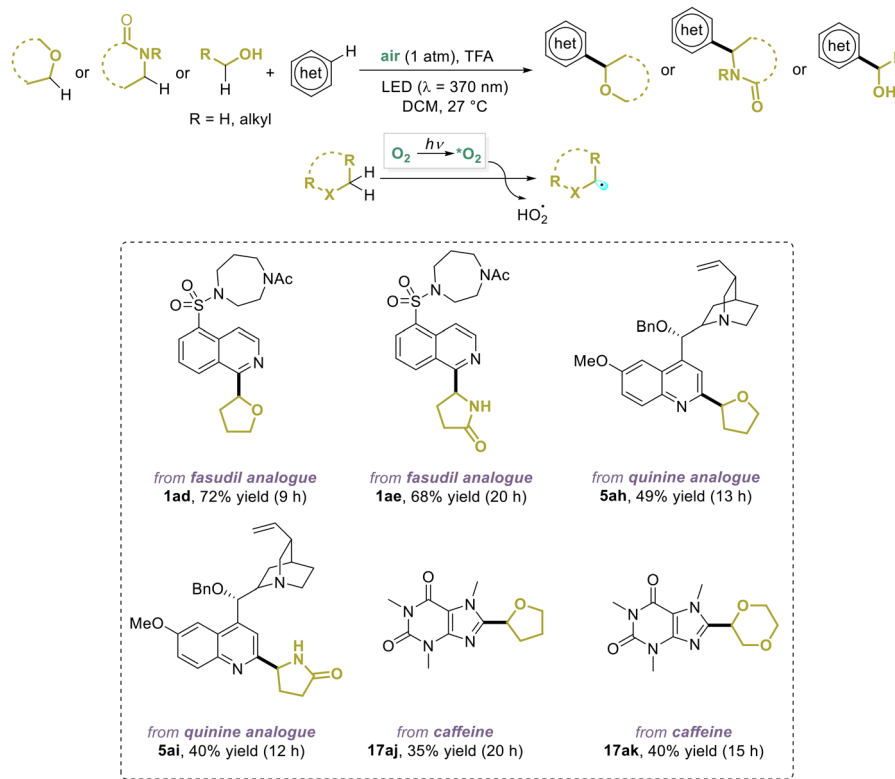


Fig. 31 Photoinduced Minisci reaction *via* aerobic oxidation of ethers, amides, and alcohols.

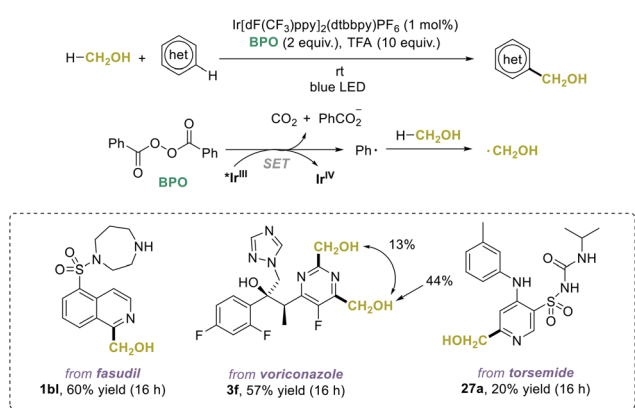


Fig. 32 Photoredox Minisci hydroxymethylation with methanol.

caffeine was modified using various aryldiazonium tetrafluoroborates, both electron-poor and electron-rich, affording **17am**–**17ax** in good yields.

## Introduction of acyl groups

Researchers have also extended Minisci-type reactions to incorporate acyl groups into diverse *N*-heteroarenes through acyl radicals, expanding the toolbox for complex molecule functionalization.

## Aldehydes as precursors

In 2023, Fang and colleagues reported a photo-induced Minisci acylation between aldehydes and purine nucleosides, showing high selectivity for the C6 position of purine (Fig. 40).<sup>93</sup> Mechanistic investigations revealed that the purine nucleoside first interacts with TFA and TBHP to form a photo-active complex, which under light irradiation, produces protonated purine nucleoside, a *tert*-butyl-oxygen radical, and a hydroxyl radical. These radicals can serve as the HAT reagent to generate acyl radicals. This method is valuable for synthesizing C6-acylated purine nucleosides that display diverse biological activities, using both aromatic and aliphatic aldehydes to yield products **11bd**–**11bz** in good yields.

## $\alpha$ -Keto acids as precursors

Drawing from the straightforward generation of radicals from carboxylic acids *via* SET and subsequent decarboxylation, in 2018, both Xia and Delord groups independently reported photo-triggered Minisci acylation with  $\alpha$ -keto acids (Fig. 41).<sup>94,95</sup> Notably, under both conditions, benzoylformic acid reacted smoothly with caffeine to afford **17a1** in moderate yields.

## Acetals as precursors

Formylated heterocycles—versatile skeletons in natural products and pharmaceuticals—can be synthesized *via* Minisci formylation. In their work in 2018, Xia and co-workers also



Fig. 33 Minisci-type alcohol-directed remote C(sp<sup>3</sup>)-H functionalization with heteroaryls via a 1,5-HAT process.



Fig. 34 Minisci-type amide-directed remote C(sp<sup>3</sup>)-H functionalization of heteroaryls via a 1,5-HAT.

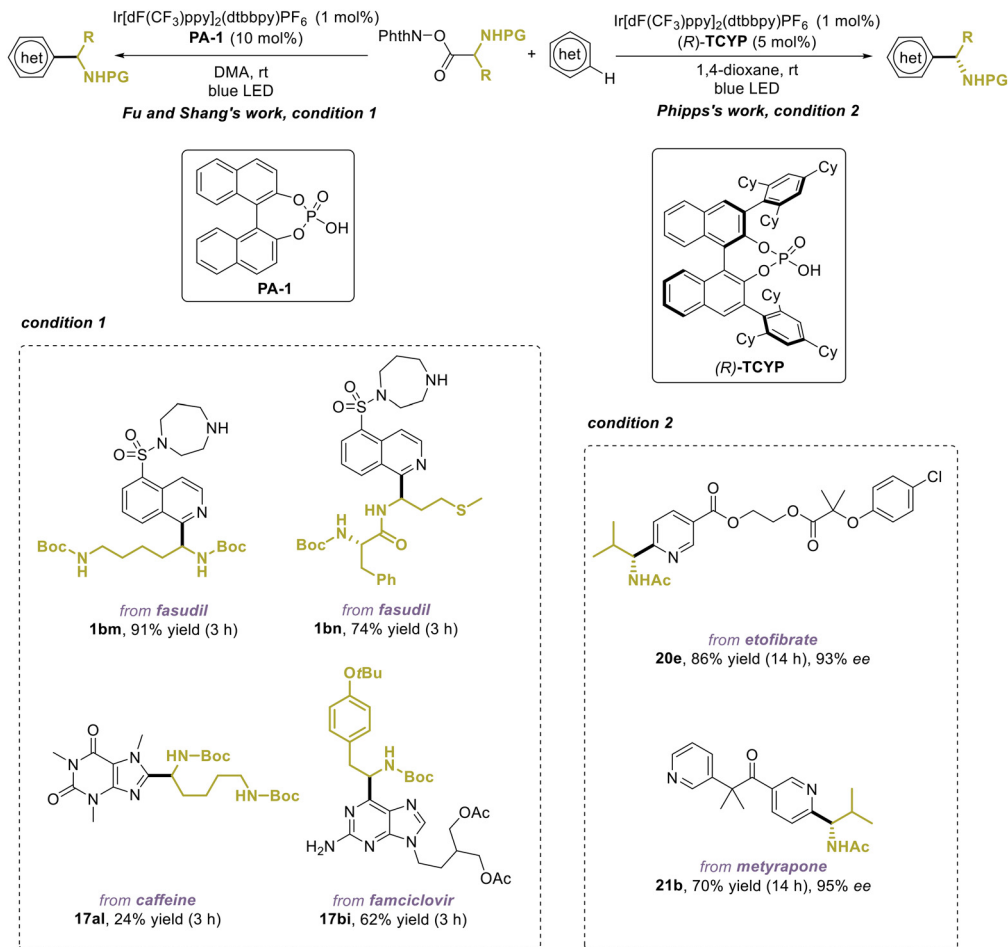


Fig. 35 Minisci  $\alpha$ -aminoalkylation of *N*-heteroarenes with NAPs.

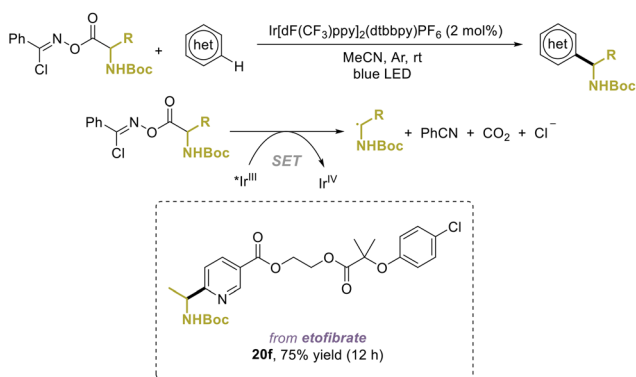


Fig. 36 Photoredox Minisci  $\alpha$ -aminoalkylation with NHBC esters.

achieved this transformation using glyoxylic acid diethyl acetal as the formyl source and  $(\text{NH}_4)_2\text{S}_2\text{O}_8$  as the oxidant, affording formylated caffeine **17a2** with 20% yield (Fig. 42, condition 1).<sup>94</sup> Then in 2020, Wang and co-workers developed an oxidant-free approach using 1,3-dioxoisindolin-2-yl 2,2-diethoxyacetate as the formyl source, which was applicable for

formylating fasudil with 60% yield (Fig. 42, condition 2).<sup>96</sup> Mechanistically, acetyl radicals are generated from the precursor *via* SET and subsequent decarboxylation and undergo the Minisci reaction then acid hydrolysis to form the desired products.

## Introduction of carbamoyl groups

In addition to acetyl and formyl groups, carbamoyl groups have also been incorporated into *N*-heteroarenes *via* Minisci-type reactions.

### Formamides as precursors

In 2016, Ji and co-workers disclosed a benzaldehyde-mediated photoredox method using formamide as the carbamoyl source and  $(\text{NH}_4)_2\text{S}_2\text{O}_8$  as a radical initiator, successfully applicable to 3-(ethoxy-carbonyl)- $\beta$ -carboline ( $\beta$ -CCE), a common scaffold in drug discovery, affording **33a** in 50% yield (Fig. 43).<sup>97</sup> Upon illumination, photoexcited benzaldehyde triggers persulfate decomposition to form sulfate radicals that subsequently gene-



Fig. 37 Photocatalytic Minisci  $\alpha$ -hydroxyalkylation with aldehydes.

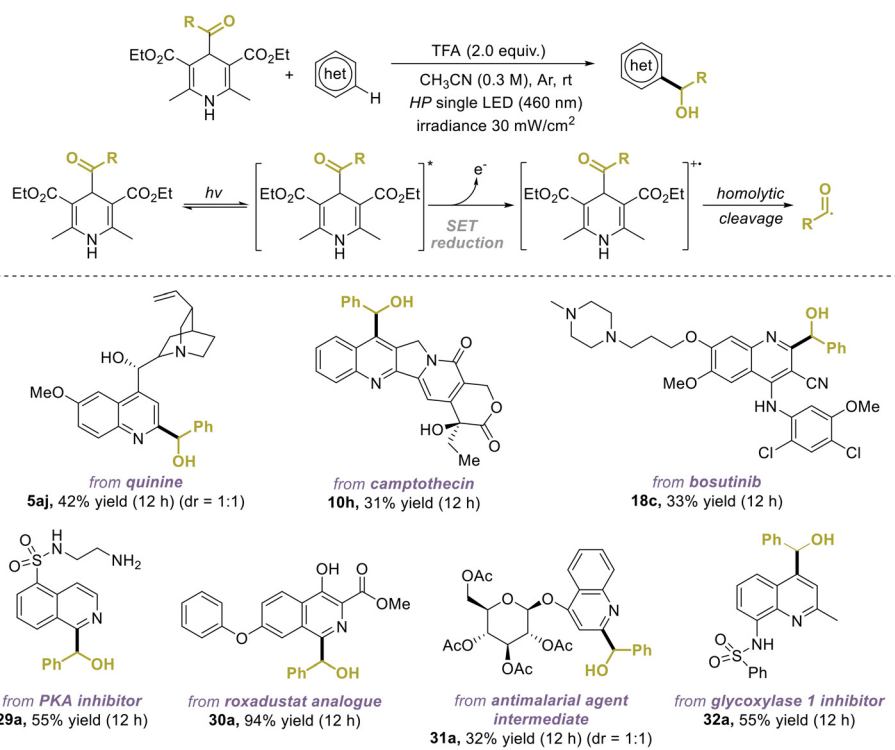


Fig. 38 Photo-mediated Minisci  $\alpha$ -hydroxyalkylation with acyl-DHPs.

rate carbamoyl radicals from formamide *via* a HAT process with formamide.

### Oxamic acids as precursors

Again, leveraging the facile radical generation from carboxylic acids, oxamic acids were employed as carbamoyl radical precursors in this transformation. In 2019, Kong and Jouffroy reported a photocatalyzed protocol using oxamic acids or pot-

assium oxamates as the carbamoyl sources, which can be applied in carbamoylating caffeine and cinchonine (Fig. 44, condition 1).<sup>98</sup> The electrophotocatalysis approach of Xu and Song in 2020 was also compatible with oxamic acids (Fig. 44, condition 2), enabling the carbamoylation of voriconazole, quinine, loratadine, tropicamide (a potent anticholinergic and muscarinic receptor antagonist), and bisacodyl (a stimulant laxative) in moderate to good yields.<sup>34</sup> In both cases, the requi-

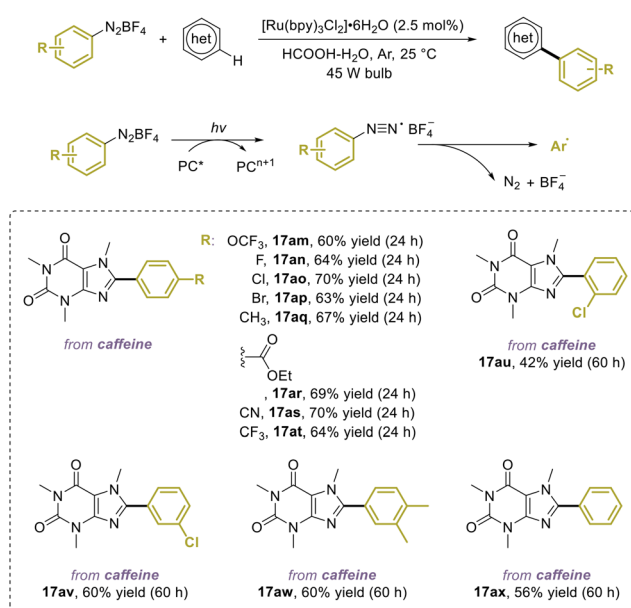


Fig. 39 Photocatalytic Minisci arylation with aryldiazonium salts.

site carbamoyl radical is generated through the SET oxidation of oxamates by the excited photocatalyst, followed by decarboxylation.

## Introduction of fluorinated groups

Small, fluorinated groups, particularly trifluoromethyl (CF<sub>3</sub>), often exert a strong impact on the physicochemical properties and biological activities of drug molecules, due to their lipophilicity, electron-withdrawing characteristic and metabolic stability.<sup>99,100</sup> It is notable that reactions involving electrophilic CF<sub>3</sub> or CF<sub>2</sub>H groups discussed here differ from conventional 'Minisci-type' chemistry but are included as they yield 'Minisci-type' products through radical addition.

### Sulfonyl chlorides and sodium sulfonates as precursors

In 2011, MacMillan and co-workers pioneered photoredox trifluoromethylation of heteroarenes using CF<sub>3</sub>SO<sub>2</sub>Cl as the

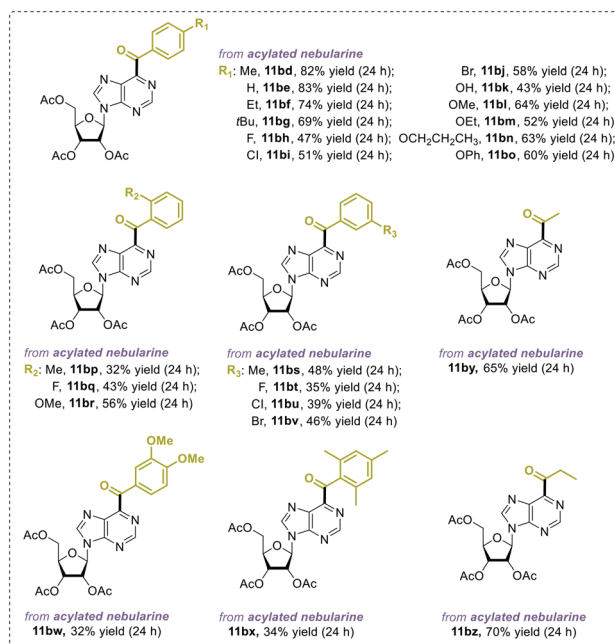
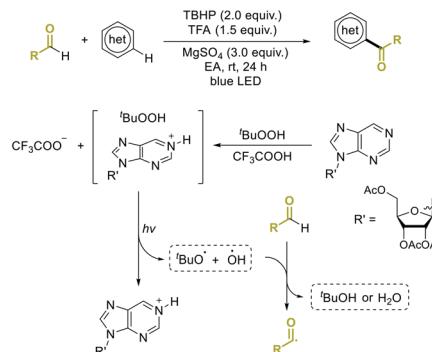


Fig. 40 Photo-induced Minisci acylation of purine nucleosides with aldehydes.

CF<sub>3</sub> source, which was effective in functionalizing a DNA base analogue, uracil, in good yield (Fig. 45).<sup>101</sup> Mechanistically, the reduction of CF<sub>3</sub>SO<sub>2</sub>Cl by the photoexcited \*Ir(III) complex followed by extrusion of SO<sub>2</sub> and the chloride anion generates CF<sub>3</sub>·, which adds to the most electron-rich position in the

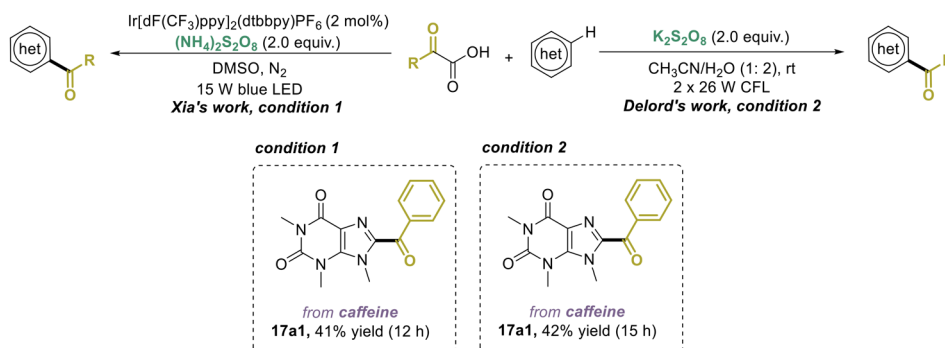


Fig. 41 Photo-triggered Minisci acylation with  $\alpha$ -keto acids.

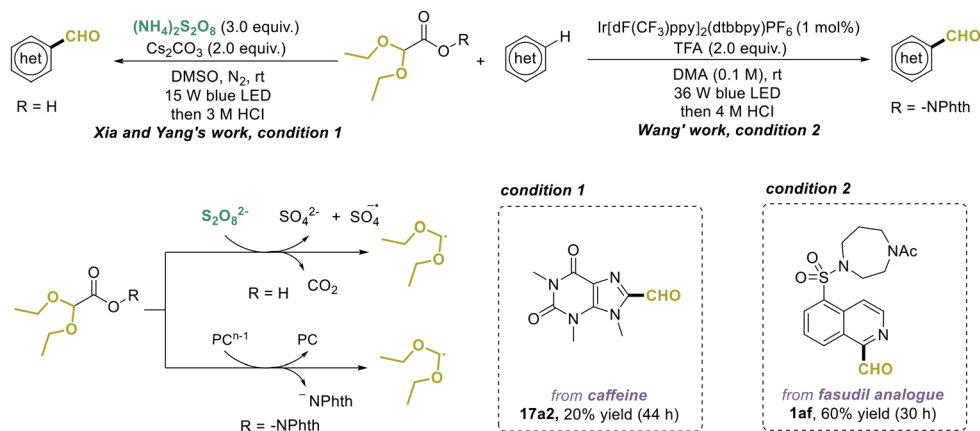


Fig. 42 Photo-mediated Minisci formylation with acetals.



Fig. 43 Benzaldehyde-mediated photocatalyzed Minisci carbamoylation with formamide.



Fig. 44 Photoredox Minisci carbamoylation with oxamic acids.

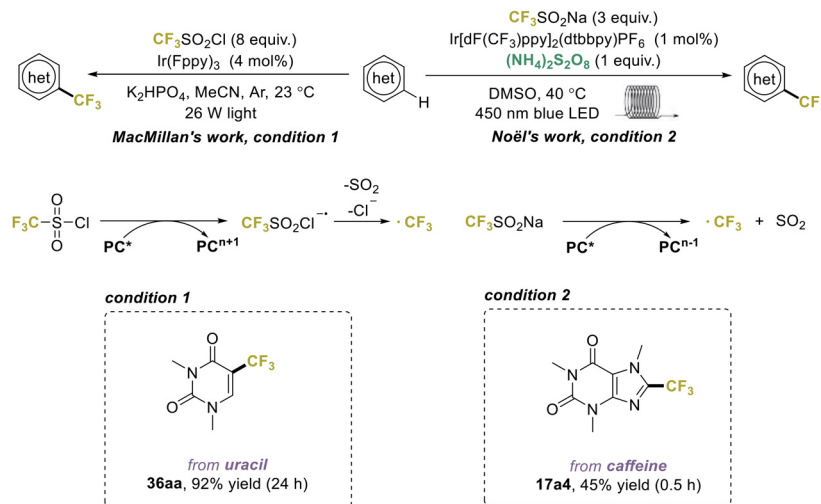


Fig. 45 Photoredox trifluoromethylation of heterocycles with  $\text{CF}_3\text{SO}_2\text{Cl}$  and  $\text{CF}_3\text{SO}_2\text{Na}$ .

*N*-heteroarene. To address cost-effectiveness and practicality in trifluoromethylations, in 2017, Noël and co-workers revealed a continuous-flow protocol using inexpensive and more stable  $\text{CF}_3\text{SO}_2\text{Na}$  (Langlois reagent) as the  $\text{CF}_3$  radical precursor

via reductive quenching of the excited photocatalyst.<sup>102</sup> Notably, this system achieved the trifluoromethylation of caffeine, yielding **17a4** in 45% yield within a residence time of 30 minutes.

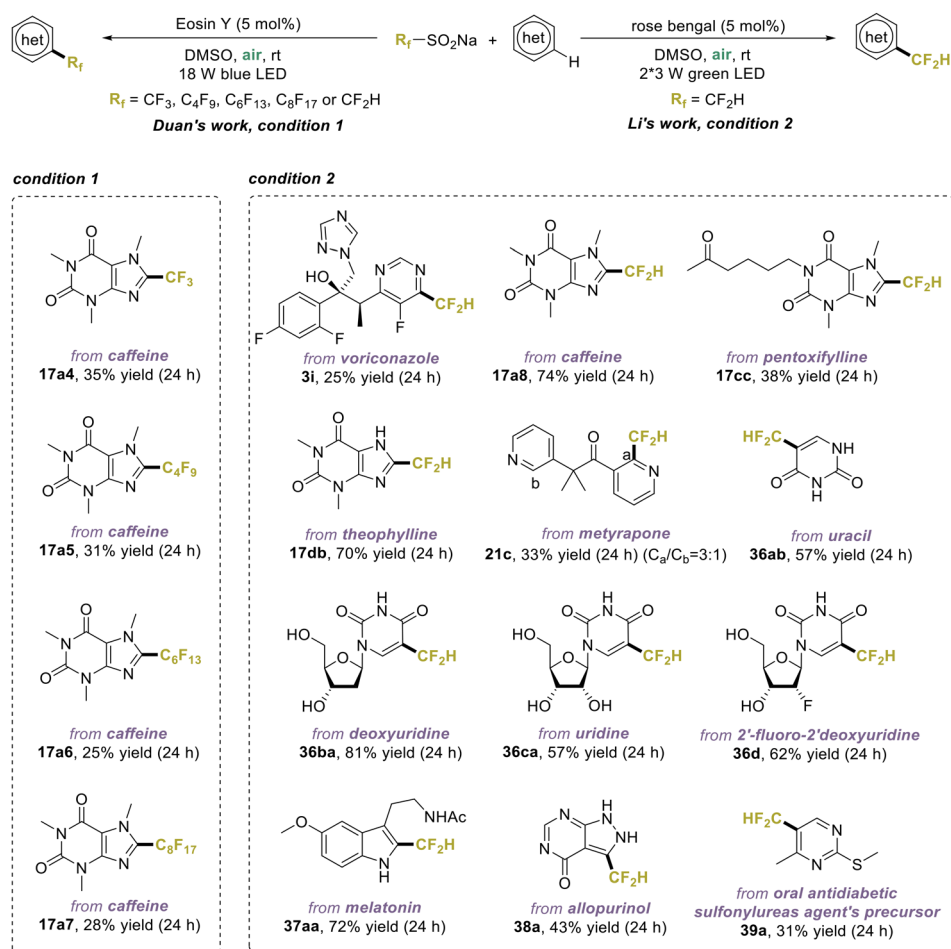


Fig. 46 Photoredox perfluoroalkylation and difluoromethylation of heterocycles with sodium sulfonates.

Building upon Noël's work, other fluorine-containing sulfinate salts have been used for photoredox perfluoroalkylation and difluoromethylation of heteroarenes under aerobic conditions, where atmospheric oxygen serves as a crucial oxidant. In 2019, Duan, Xia, and co-workers utilized sodium perfluoroalkanesulfonates with eosin Y as the photocatalyst, enabling perfluoroalkylation of caffeine with  $C_4F_9SO_2Na$ ,  $C_6F_{13}SO_2Na$ , and  $C_8F_{17}SO_2Na$  to afford products **17a4–17a7** with 25–35%

yields (Fig. 46, condition 1).<sup>103</sup> Furthermore, in 2020, recognizing the substantial potential of the difluoromethyl ( $CF_2H$ ) group in drug scaffolds, Li, Meng, and colleagues disclosed a difluoromethylation using  $CF_2HSO_2Na$  as the  $CF_2H$  source and rose bengal as the photocatalyst (Fig. 46, condition 2).<sup>104</sup> This protocol was effective in the LSF of complex nitrogen-containing bioactive molecules, including purine-based species like caffeine, pentoxifylline, and theophylline, furnishing **17a8**,

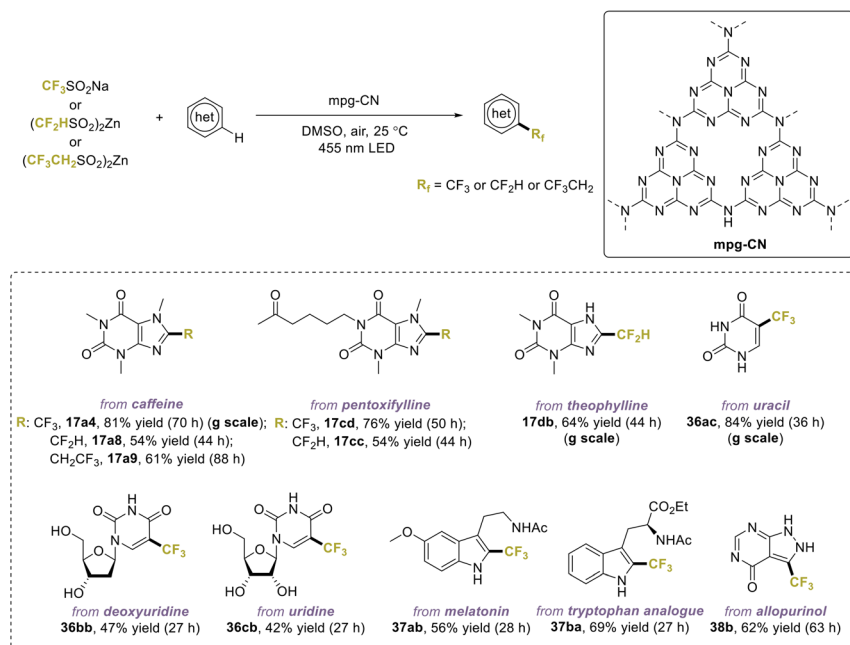


Fig. 47 Organic semiconductor photoredox fluoroalkylation of heterocycles.



Fig. 48 Photoredox trifluoromethylation of heterocycles with TFAA and Tf<sub>2</sub>O.



**Fig. 49** Photocatalyzed difluoroacetamidation of *N*-heteroarenes with bromodifluoroacetamides.

**17ce** and **17db** with selective functionalization in the imidazole moiety and moderate to good yields. Notably, the difluoromethylated product **36ba**, derived from deoxyuridine, exhibits promising anti-cancer activity against some cancer cell lines. In addition to transition metal complexes and organic dyes as photocatalysts, König and Antonietti introduced mesoporous graphitic carbon nitride (mpg-CN) as a heterogeneous semiconductor catalyst for the late-stage fluoroalkylation of heteroarenes in 2019 (Fig. 47).<sup>105</sup> Using Langlois reagent or zinc sulfonates as fluoroalkyl radical precursors,

various pharmaceuticals and bioactive molecules with purine, pyrimidine, and indole cores displayed good reactivity in trifluoromethylation, difluoromethylation, and 2,2,2-trifluoroethylation. Notably, this protocol demonstrated excellent scalability, enabling efficient reactions on a gram scale, exemplified by successful synthesis of **17a4**, **17db** and **36aa**.

### Anhydrides as precursors

In 2015, the use of trifluoroacetic anhydride (TFAA) as the CF<sub>3</sub> radical precursor was reported by Stephenson and co-workers, using pyridine *N*-oxide as an electron-poor auxiliary to facilitate the mild decarboxylation of TFAA *via* formation of reducible intermediate ( $E_1^{\text{red}} = -1.10$  V *versus* SCE) (Fig. 48, condition 1).<sup>106</sup> Reduction of the intermediate by a common photoredox catalyst, such as Ru(bpy)<sub>3</sub>, and the subsequent extrusion of pyridine and CO<sub>2</sub> generate CF<sub>3</sub> radicals. Notably, a gram-scale trifluoromethylation of caffeine was achieved with 54% yield. Similarly, in 2018, Qing and co-workers utilized trifluoromethanesulfonic anhydride (Tf<sub>2</sub>O) as the CF<sub>3</sub> radical precursor with pyridine as the activating reagent, forming a reducible pyridinium complex (Fig. 48, condition 2).<sup>107</sup> This protocol effectively trifluoromethylated pentoxifylline, affording **17cd** in a 50% yield.

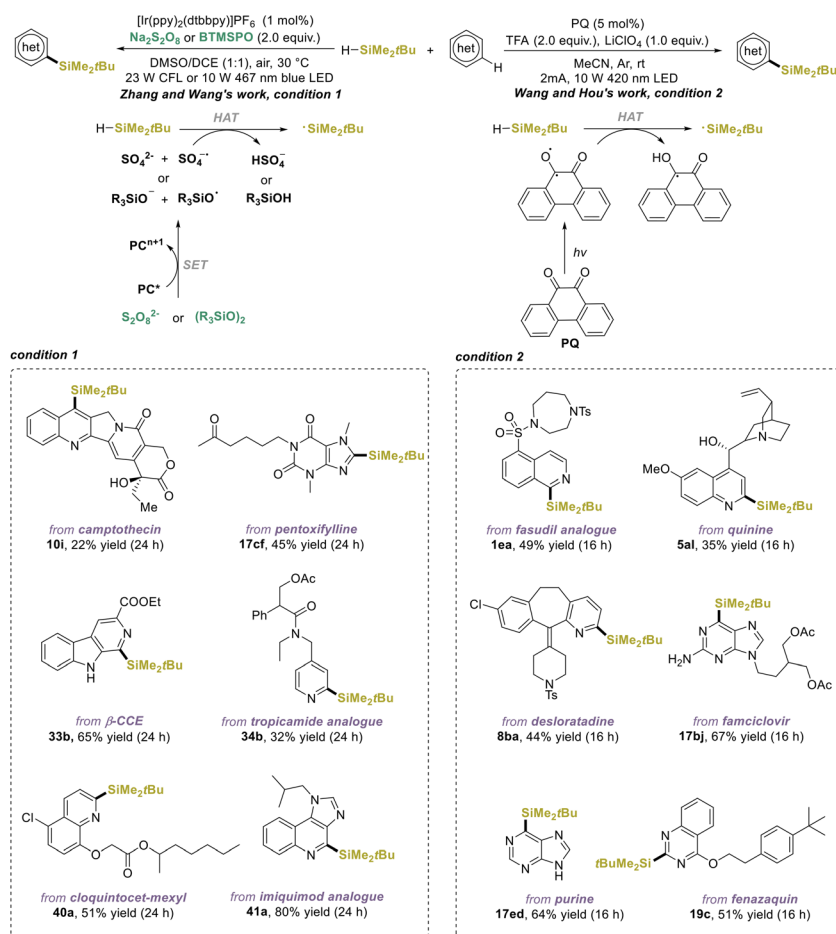


**Fig. 50** Photocatalyzed Minisci silylation with trialkylhydrosilanes.



Fig. 51 Photoredox Minisci borylation with amine-boranes.

### Bromides as precursors

The incorporation of a difluoroacetamide moiety on *N*-heteroarenes can be achieved by using bromodifluoroacetamides as electrophilic  $\alpha$ -difluoroacetyl radical sources through photocatalysis, as disclosed by Liu and co-workers in 2014 (Fig. 49).<sup>108</sup> This protocol is applicable to complex hetero-

aromatics, as exemplified by the successful functionalization of pentoxifylline with 82% yield.

## Introduction of trialkylsilyl groups

The potential of heteroaryltrialkylsilanes as promising therapeutic agents has sparked considerable interest in their synthesis.<sup>109,110</sup> In 2019, Zhang, Wang and co-workers developed a photocatalytic Minisci silylation approach with trialkylhydrosilanes (Fig. 50, condition 1), effectively enabling the silylation of complex molecules like camptothecin, pentoxifylline, carboline, tropicamide analogue, cloquintocet-mexyl, and imiquimod analogue, using radical initiators  $\text{Na}_2\text{S}_2\text{O}_8$ , bis(trimethylsilyl)peroxide (BTMSP), or  $\text{iPr}_3\text{SiSH}$ .<sup>111</sup> More recently, in 2023, Wang, Hou and co-workers reported an organoelectro-photocatalytic approach using *tert*-butyldimethylsilane as the silyl source and 9,10-phenanthrenequinone (PQ) as both the organophotosensitizer and HAT reagent, where silyl radicals are generated *via* a HAT process between the excited PQ and silanes (Fig. 50, condition 2).<sup>112</sup> Notably, this strategy is applicable to the late-stage silylation of bioactive molecules, including the fasudil analogue, quinine, desloratadine, famciclovir, purine, and fenazaquin.

## Introduction of boron functional groups

The introduction of boron groups to *N*-heteroarenes is highly promising due to their significance as building blocks in synthetic chemistry and potential drug candidates in medicinal



Fig. 52 Photoredox Minisci glycosylation with glycosyl bromides.

chemistry.<sup>113</sup> In 2021, Leonori and co-workers introduced a photoredox Minisci borylation strategy using simple amine-borane reagents as boryl radical precursors,  $(\text{NH}_4)_2\text{S}_2\text{O}_8$  as the HAT reagent, and 4CzIPN as the photocatalyst (Fig. 51).<sup>114</sup> Boryl radicals are generated through a polarity-matched HAT process of amine-borane with sulfate radical anion. This method is applicable to the borylation of complex pharmaceuticals and agrochemicals, including fasudil, fasudil analogue, quinoxifen, voriconazole, cinchonine, and famciclovir.

## Introduction of glycosyl groups

*C*-Glycosyl compounds, valued for their stability and potential in drug discovery, are a focus of interest.<sup>115</sup> In 2021, Yu and co-workers revealed a photoredox Minisci glycosylation using glycosyl bromides to synthesize potential *C*-nucleoside analogues with anticancer or antiviral properties (Fig. 52).<sup>116</sup> Mechanistically, the reaction is initiated by SET with the photoexcited  $^*\text{Ir}(\text{III})$  complex with  $\text{Et}_3\text{N}$  to give  $\text{Ir}(\text{II})$  and  $\text{Et}_3\text{N}^{+\bullet}$ . Then galactosyl bromides are reduced by  $\text{Ir}(\text{II})$  to give galactosyl

radicals, which perform nucleophilic attack on *N*-heteroarenes, followed by oxidation and deprotonation with  $\text{Et}_3\text{N}^{+\bullet}$  to produce the final *C*-nucleoside analogues. His method exhibits  $\alpha$ -stereoselectivity and allows for the direct galactosylation of biologically relevant molecules like nebularine, famciclovir, theophylline, and adenine.

## Summary and outlook

This review highlights diverse approaches for photo-induced Minisci-type reactions in the LSF of *N*-heteroarenes, revealing significant advancements in radical generation—alkyl, aryl, acyl, carbamoyl, fluoroalkyl, boryl, silyl and glycosyl—from various precursors under photoirradiation since Dunston's review in 2011 (Fig. 53).<sup>6</sup> Recognizing the established power and versatility of LSF methodologies in drug discovery, it is evident that these photocatalyzed Minisci-type reactions will play a pivotal role in accelerating drug discovery in the future.

While considerable strides have been made in advancing Minisci-type reactions for LSF of pharmaceutically relevant compounds, several challenges underscore the need for

Functional group	Radical precursors
alkyl and cycloalkyl groups	$\text{R}-\text{H}$ $\text{R}-\text{Br}$ $\text{R}-\text{I}$ $\text{R}-\text{OH}$ $\text{R}-\text{CHO}$ $\text{R}-\text{COOH}$ $\text{R}-\text{B}(\text{OH})_2$ $\text{R}-\text{BF}_3\text{K}$ 
$\alpha$ -oxyalkyl, $\alpha$ -aminoalkyl, and $\alpha$ -hydroxyalkyl groups	
aryl groups	$\text{Ar}-\text{N}_2\text{BF}_4$
acyl groups	
carbamoyl groups	$\text{H}-\text{CONH}_2$ $\text{XO}-\text{C}(=\text{O})-\text{N}(\text{R}^1)(\text{R}^2)$
fluorinated groups	$\text{CF}_3\text{SO}_2\text{Cl}$ $\text{R}_f-\text{SO}_2\text{Na}$ $(\text{R}_f\text{SO}_2)_2\text{Zn}$ $\text{F}_3\text{C}-\text{SO}_2-\text{O}-\text{SO}_2-\text{CF}_3$ $\text{F}_3\text{C}-\text{C}(=\text{O})-\text{O}-\text{C}(=\text{O})-\text{CF}_3$ $\text{Br}-\text{C}(=\text{O})-\text{N}(\text{R}^1)(\text{R}^2)$
trialkylsilyl groups	$\text{H}-\text{SiMe}_2\text{tBu}$
boryl groups	$\text{H}-\text{BH}_2\text{NMe}_3$
glycosyl groups	

Fig. 53 Overview of diverse approaches for photo-induced Minisci-type reactions in the LSF of *N*-heteroarenes.

further exploration and innovation to fully unlock the tremendous potential of Minisci-type reactions in drug discovery. First, achieving good regioselectivity remains a hurdle, particularly for complex natural skeletons with multiple reactive sites which often result in the formation of regioisomers and multisubstituted products. The second challenge pertains to achieving enantioselectivity, a critical aspect given the prevalence of chiral centres in biologically active molecules. Despite the development of some enantioselective variants,<sup>11</sup> their application to complex molecules remains limited. Additionally, our review reveals a concentration on specific substrates, such as pyridine, quinoline, isoquinoline, and purine moieties, while neglecting the modification of other heterocycles commonly found in pharmaceuticals and alkaloids. Lastly, the lack of standardized setups and difficulties in scaling-up of the photocatalysis methodology pose potential hurdles in the process development in drug discovery, emphasizing the need for the development of advanced technologies. Scrutinizing these limitations is crucial, particularly for identifying the current gaps in knowledge and laying the foundation for future research directions.

Looking ahead, as organic chemistry continues to evolve dynamically, the integration of technological advancements, such as flow apparatuses and high-throughput platforms, holds promise for addressing these challenges. We anticipate a future where prospective drug candidates can undergo established LSF procedures, offering substantial cost and time savings for practitioners in both academia and the pharmaceutical industry.

## Author contributions

Conceptualization, F. Qiu, J. Wu and P. Jia; investigation, X. Zhang and S. Li; writing – original draft, X. Zhang, S. Li and P. Jia; writing – review and editing, X. Zhang, H.T. Ang, J. Wu and P. Jia; project administration, P. Jia; supervision, J. Wu and P. Jia.

## Conflicts of interest

There are no conflicts to declare.

## Acknowledgements

We are grateful for the financial support from the National Natural Science Foundation of China (no. 22201214) and the Scientific Research Project of Tianjin Education Commission (no. 2021KJ125).

## References

- 1 F. Minisci, R. Galli, M. Cecere, V. Malatesta and T. Caronna, *Tetrahedron Lett.*, 1968, **9**, 5609–5612.
- 2 F. Minisci, R. Galli, V. Malatesta and T. Caronna, *Tetrahedron*, 1970, **26**, 4083–4091.
- 3 F. Minisci, R. Bernardi, F. Bertini, R. Galli and M. Perchinummo, *Tetrahedron*, 1971, **27**, 3575–3579.
- 4 F. Minisci, E. Vismara and F. Fontana, *Heterocycles*, 1989, **28**, 489–519.
- 5 F. Minisci, F. Fontana and E. Vismara, *J. Heterocycl. Chem.*, 1990, **2**, 79–96.
- 6 M. A. J. Duncton, *MedChemComm*, 2011, **2**, 1135–1161.
- 7 J. Tauber, D. Imbri and T. Opatz, *Molecules*, 2014, **19**, 16190.
- 8 R. S. J. Proctor and R. J. Phipps, *Angew. Chem., Int. Ed.*, 2019, **58**, 13666–13699.
- 9 J. Dong, Y. Liu and Q. Wang, *Chin. J. Org. Chem.*, 2021, **41**, 3771–3791.
- 10 W. Wang and S. Wang, *Curr. Org. Chem.*, 2021, **25**, 894–934.
- 11 P. D. Bacos, A. S. K. Lahdenperä and R. J. Phipps, *Acc. Chem. Res.*, 2023, **56**, 2037–2049.
- 12 M. Baumann and I. R. Baxendale, *Beilstein J. Org. Chem.*, 2013, **9**, 2265–2319.
- 13 N. Kerru, L. Gummidi, S. Maddila, K. K. Gangu and S. B. A. Jonnalagadda, *Molecules*, 2020, **25**, 1909.
- 14 M. M. Heravi and V. Zadsirjan, *RSC Adv.*, 2020, **10**, 44247–44311.
- 15 E. Vitaku, D. T. Smith and J. T. Njardarson, *J. Med. Chem.*, 2014, **57**, 10257–10274.
- 16 P. Bhutani, G. Joshi, N. Raja, N. Bachhav, P. K. Rajanna, H. Bhutani, A. T. Paul and R. Kumar, *J. Med. Chem.*, 2021, **64**, 2339–2381.
- 17 T. Cernak, K. D. Dykstra, S. Tyagarajan, P. Vachal and S. W. Krska, *Chem. Soc. Rev.*, 2016, **45**, 546–576.
- 18 J. Borgel and T. Ritter, *Chem*, 2020, **6**, 1877–1887.
- 19 R. Cannalire, S. Pelliccia, L. Sancineto, E. Novellino, G. C. Tron and M. Giustiniano, *Chem. Soc. Rev.*, 2021, **50**, 766–897.
- 20 L. Guillemard, N. Kaplaneris, L. Ackermann and M. J. Johansson, *Nat. Rev. Chem.*, 2021, **5**, 522–545.
- 21 F. Minisci, E. Vismara, F. Fontana, G. Morini, M. Serravalle and C. Giordano, *J. Org. Chem.*, 1987, **52**, 730–736.
- 22 F. O'Hara, D. G. Blackmond and P. S. Baran, *J. Am. Chem. Soc.*, 2013, **135**, 12122–12134.
- 23 C. K. Prier, D. A. Rankic and D. W. C. MacMillan, *Chem. Rev.*, 2013, **113**, 5322–5363.
- 24 N. A. Romero and D. A. Nicewicz, *Chem. Rev.*, 2016, **116**, 10075–10166.
- 25 L. Marzo, S. K. Pagire, O. Reiser and B. König, *Angew. Chem., Int. Ed.*, 2018, **57**, 10034–10072.
- 26 F. Strieth-Kalthoff, M. J. James, M. Teders, L. Pitzer and F. Glorius, *Chem. Soc. Rev.*, 2018, **47**, 7190–7202.
- 27 R. C. McAtee, E. J. McClain and C. R. J. Stephenson, *Trends Chem.*, 2019, **1**, 111–125.
- 28 Q.-Q. Zhou, Y.-Q. Zou, L.-Q. Lu and W.-J. Xiao, *Angew. Chem., Int. Ed.*, 2019, **58**, 1586–1604.
- 29 G. E. M. Crisenza, D. Mazzarella and P. Melchiorre, *J. Am. Chem. Soc.*, 2020, **142**, 5461–5476.
- 30 J. Xuan, Z.-G. Zhang and W.-J. Xiao, *Angew. Chem., Int. Ed.*, 2015, **54**, 15632–15641.

- 31 R. A. Garza-Sanchez, A. Tlahuext-Aca, G. Tavakoli and F. Glorius, *ACS Catal.*, 2017, **7**, 4057–4061.
- 32 J. Wang, G. Li, G. He and G. Chen, *Asian J. Org. Chem.*, 2018, **7**, 1307–1310.
- 33 J. Genovino, Y. Lian, Y. Zhang, T. O. Hope, A. Juneau, Y. Gagné, G. Ingle and M. Frenette, *Org. Lett.*, 2018, **20**, 3229–3232.
- 34 X.-L. Lai, X.-M. Shu, J. Song and H.-C. Xu, *Angew. Chem., Int. Ed.*, 2020, **59**, 10626–10632.
- 35 T. C. Sherwood, N. Li, A. N. Yazdani and T. G. M. Dhar, *J. Org. Chem.*, 2018, **83**, 3000–3012.
- 36 W.-M. Cheng, R. Shang, M.-C. Fu and Y. Fu, *Chem. – Eur. J.*, 2017, **23**, 2537–2541.
- 37 L. M. Kammer, A. Rahman and T. Opatz, *Molecules*, 2018, **23**, 764–779.
- 38 M.-C. Fu, R. Shang, B. Zhao, B. Wang and Y. Fu, *Science*, 2019, **363**, 1429–1434.
- 39 X. L. Lyu, S. S. Huang, H. J. Song, Y. X. Liu and Q. M. Wang, *Org. Lett.*, 2019, **21**, 5728–5732.
- 40 S. Jin, X. Geng, Y. Li and K. Zheng, *Eur. J. Org. Chem.*, 2021, 969.
- 41 J. Li, S. S. Tan, S. H. Kyne and P. W. H. Chan, *Adv. Synth. Catal.*, 2022, **364**, 802–810.
- 42 D. A. DiRocco, K. Dykstra, S. Krska, P. Vachal, D. V. Conway and M. Tudge, *Angew. Chem., Int. Ed.*, 2014, **53**, 4802–4806.
- 43 J. Jin and D. W. C. MacMillan, *Nature*, 2015, **525**, 87–90.
- 44 X. Hu, G.-X. Li, G. He and G. Chen, *Org. Chem. Front.*, 2019, **6**, 3205–3209.
- 45 Y. Wang, L. Yang, S. Liu, L. Huang and Z.-Q. Liu, *Adv. Synth. Catal.*, 2019, **361**, 4568–4574.
- 46 Z. Cao, M. Ji, X. Wang, X. Wu, Y. Li and C. Zhu, *Green Chem.*, 2022, **24**, 4498–4503.
- 47 S. P. Pitre, M. Muuronen, D. A. Fishman and L. E. Overman, *ACS Catal.*, 2019, **9**, 3413–3418.
- 48 J. Dong, Z. Wang, X. Wang, H. Song, Y. Liu and Q. Wang, *J. Org. Chem.*, 2019, **84**, 7532–7540.
- 49 J. Dong, Z. Wang, X. Wang, H. Song, Y. Liu and Q. Wang, *Sci. Adv.*, 2019, **5**, eaax9955.
- 50 Z. Wang, Q. Liu, X. Ji, G. Deng and H. Huang, *ACS Catal.*, 2020, **10**, 154–159.
- 51 Z. Wang, X. Ji, J. Zhao and H. Huang, *Green Chem.*, 2019, **21**, 5512–5516.
- 52 X. Wang, X. Shao, Z. Cao, X. Wu and C. Zhu, *Adv. Synth. Catal.*, 2022, **364**, 1200–1204.
- 53 Á. Gutiérrez-Bonet, C. Remeur, J. K. Matsui and G. A. Molander, *J. Am. Chem. Soc.*, 2017, **139**, 12251–12258.
- 54 J. Dong, F. Yue, W. Xu, H. Song, Y. Liu and Q. Wang, *Green Chem.*, 2020, **22**, 5599–5604.
- 55 I. B. Seiple, S. Su, R. A. Rodriguez, R. Gianatassio, Y. Fujiwara, A. L. Sobel and P. S. Baran, *J. Am. Chem. Soc.*, 2010, **132**, 13194–13196.
- 56 G.-X. Li, C. A. Morales-Rivera, Y. Wang, F. Gao, G. He, P. Liu and G. Chen, *Chem. Sci.*, 2016, **7**, 6407–6412.
- 57 J. Dong, F. Yue, H. Song, Y. Liu and Q. Wang, *Chem. Commun.*, 2020, **56**, 12652–12655.
- 58 G. A. Molander, V. Colombel and V. A. Braz, *Org. Lett.*, 2011, **13**, 1852–1855.
- 59 J. K. Matsui, D. N. Primera and G. A. Molander, *Chem. Sci.*, 2017, **8**, 3512–3522.
- 60 H. Yan, Z.-W. Hou and H.-C. Xu, *Angew. Chem., Int. Ed.*, 2019, **58**, 4592–4595.
- 61 J. Li, C.-Y. Huang, J.-T. Han and C.-J. Li, *ACS Catal.*, 2021, **11**, 14148–14158.
- 62 P. Nuhant, M. S. Oderinde, J. Genovino, A. Juneau, Y. Gagné, C. Allais, G. M. Chinigo, C. Choi, N. W. Sach, L. Bernier, Y. M. Fobian, M. W. Bundesmann, B. Khunte, M. Frenette and O. O. Fadeyi, *Angew. Chem., Int. Ed.*, 2017, **56**, 15309–15313.
- 63 J. Dong, X. Lyu, Z. Wang, X. Wang, H. Song, Y. Liu and Q. Wang, *Chem. Sci.*, 2019, **10**, 976–982.
- 64 J. J. Perkins, J. W. Shubert, E. C. Streckfuss, J. Balsells and A. ElMarrouni, *Eur. J. Org. Chem.*, 2020, 1515–1522.
- 65 H. Cao, X. Tang, H. Tang, Y. Yuan and J. Wu, *Chem. Catal.*, 2021, **1**, 523–598.
- 66 C.-Y. Huang, J. Li, W. Liu and C.-J. Li, *Chem. Sci.*, 2019, **10**, 5018–5024.
- 67 X.-A. Liang, L. Niu, S. Wang, J. Liu and A. Lei, *Org. Lett.*, 2019, **21**, 2441–2444.
- 68 H. Zhao and J. Jin, *Org. Lett.*, 2019, **21**, 6179–6184.
- 69 H. Zhao, Z. Li and J. Jin, *New J. Chem.*, 2019, **43**, 12533–12537.
- 70 Y.-R. Luo, *Handbook of Bond Dissociation Energies in Organic Compounds*. CRC, Boca Raton, 2002.
- 71 P. Xu, P.-Y. Chen and H.-C. Xu, *Angew. Chem., Int. Ed.*, 2020, **59**, 14275–14280.
- 72 C.-Y. Huang, J. Li and C.-J. Li, *Nat. Commun.*, 2021, **12**, 4010.
- 73 J. Xu, H. Cai, J. Shen, C. Shen, J. Wu, P. Zhang and X. Liu, *J. Org. Chem.*, 2021, **86**, 17816–17832.
- 74 H. Tian, H. Yang, C. Tian, G. An and G. Li, *Org. Lett.*, 2020, **22**, 7709–7715.
- 75 D.-S. Li, T. Liu, Y. Hong, C.-L. Cao, J. Wu and H.-P. Deng, *ACS Catal.*, 2022, **12**, 4473–4480.
- 76 J. Jin and D. W. C. MacMillan, *Angew. Chem., Int. Ed.*, 2015, **54**, 1565–1569.
- 77 J.-Y. Dong, Q. Xia, X.-L. Luy, C.-C. Yan, H.-J. Song, Y.-X. Liu and Q.-M. Wang, *Org. Lett.*, 2018, **20**, 5661–5665.
- 78 R. Grainger, T. D. Heightman, S. V. Ley, F. Lima and C. N. Johnson, *Chem. Sci.*, 2018, **10**, 2264–2271.
- 79 M. Bhakat, P. Biswas, J. Dey and J. Guin, *Org. Lett.*, 2021, **23**, 6886–6890.
- 80 C. A. Huff, R. D. Cohen, K. D. Dykstra, E. Streckfuss, D. A. DiRocco and S. W. Krska, *J. Org. Chem.*, 2016, **81**, 6980–6987.
- 81 X. Wu, H. Zhang, N. Tang, Z. Wu, D. Wang, M. Ji, Y. Xu, M. Wang and C. Zhu, *Nat. Commun.*, 2018, **9**, 3343.
- 82 Z. Cao, M. Ji, X. Wang, X. Wu, Y. Li and C. Zhu, *Green Chem.*, 2022, **24**, 4498–4503.

- 83 G.-X. Li, X. Hu, G. He and G. Chen, *Chem. Sci.*, 2019, **10**, 688–693.
- 84 H. Chen, W. Fan, X.-A. Yuan and S. Yu, *Nat. Commun.*, 2019, **10**, 4743.
- 85 Z. Deng, G.-X. Li, G. He and G. Chen, *J. Org. Chem.*, 2019, **84**, 15777–15787.
- 86 W.-M. Cheng, R. Shang and Y. Fu, *ACS Catal.*, 2017, **7**, 907–911.
- 87 R. S. J. Proctor, H. J. Davis and R. J. Phipps, *Science*, 2018, **360**, 419–422.
- 88 X. Li, Q. Zhang, W. Zhang, Y. Wang and Y. Pan, *J. Org. Chem.*, 2019, **84**, 14360–14368.
- 89 H. Fuse, H. Nakao, Y. Saga, A. Fukatsu, M. Kondo, S. Masaoka, H. Mitsunuma and M. Kanai, *Chem. Sci.*, 2020, **11**, 12206–12211.
- 90 B. Bieszczad, L. A. Perego and P. Melchiorre, *Angew. Chem., Int. Ed.*, 2019, **58**, 16878–16883.
- 91 J. Yamaguchi, A. D. Yamaguchi and K. Itami, *Angew. Chem., Int. Ed.*, 2012, **51**, 8960–9009.
- 92 D. Xue, Z.-H. Jia, C.-J. Zhao, Y.-Y. Zhang, C. Wang and J. Xiao, *Chem. – Eur. J.*, 2014, **20**, 2960–2965.
- 93 L. Li, H. Zheng, F. Guo, Z. Fang, Q. Sun, J. Li, Q. Gao, T. Zhang and L. Fang, *Chem. Commun.*, 2023, **59**, 3910–3913.
- 94 W. Jia, Y. Jian, B. Huang, C. Yang and W. Xia, *Synlett*, 2018, **29**, 1881–1886.
- 95 L. Guillemard, F. Colobert and J. Wencel-Delord, *Adv. Synth. Catal.*, 2018, **360**, 4184–4190.
- 96 J. Dong, X. Wang, H. Song, Y. Liu and Q. Wang, *Adv. Synth. Catal.*, 2020, **362**, 2155–2159.
- 97 Y. Zhang, K. B. Teuscher and H. Ji, *Chem. Sci.*, 2016, **7**, 2111–2118.
- 98 M. Jouffroy and J. Kong, *Chem. – Eur. J.*, 2019, **25**, 2217–2221.
- 99 T. Liang, C. N. Neumann and T. Ritter, *Angew. Chem., Int. Ed.*, 2013, **52**, 8214–8264.
- 100 J. Wang, M. Sánchez-Roselló, J. L. Aceña, C. del Pozo, A. E. Sorochinsky, S. Fustero, V. A. Soloshonok and H. Liu, *Chem. Rev.*, 2014, **114**, 2432–2506.
- 101 D. A. Nagib and D. W. C. MacMillan, *Nature*, 2011, **480**, 224–228.
- 102 I. Abdiaj, C. Bottecchia, J. Alcazar and T. Noël, *Synthesis*, 2017, **49**, 4978–4985.
- 103 Z. Wei, S. Qi, Y. Xu, H. Liu, J. Wu, H. Li, C. Xia and G. Duan, *Adv. Synth. Catal.*, 2019, **361**, 5490–5498.
- 104 W. Zhang, X.-X. Xiang, J. Chen, C. Yang, Y.-L. Pan, J.-P. Cheng, Q. Meng and X. Li, *Nat. Commun.*, 2020, **11**, 638.
- 105 I. Ghosh, J. Khamrai, A. Savateev, N. Shlapakov, M. Antonietti and B. König, *Science*, 2019, **365**, 360–366.
- 106 J. W. Beatty, J. J. Douglas, K. P. Cole and C. R. J. Stephenson, *Nat. Commun.*, 2015, **6**, 7919.
- 107 Y. Ouyang, X. H. Xu and F. L. Qing, *Angew. Chem., Int. Ed.*, 2018, **57**, 6926–6929.
- 108 L. Wang, X.-J. Wei, W.-L. Jia, J.-J. Zhong, L.-Z. Wu and Q. Liu, *Org. Lett.*, 2014, **16**, 5842–5845.
- 109 A. K. Franz and S. O. Wilson, *J. Med. Chem.*, 2013, **56**, 388–405.
- 110 R. Ramesh and D. S. Reddy, *J. Med. Chem.*, 2018, **61**, 3779–3798.
- 111 S. Liu, P. Pan, H. Fan, H. Li, W. Wang and Y. Zhang, *Chem. Sci.*, 2019, **10**, 3817–3825.
- 112 Q. Wan, Z.-W. Hou, X.-R. Zhao, X. Xie and L. Wang, *Org. Lett.*, 2023, **25**, 1008–1013.
- 113 I. A. I. Mkhaliid, J. H. Barnard, T. B. Marder, J. M. Murphy and J. F. Hartwig, *Chem. Rev.*, 2010, **110**, 890–931.
- 114 J. H. Kim, T. Constantin, M. Simonetti, J. Llaveria, N. S. Sheikh and D. Leonori, *Nature*, 2021, **595**, 677–683.
- 115 É. Bokor, S. Kun, D. Goyard, M. Tóth, J.-P. Praly, S. Vidal and L. Somsák, *Chem. Rev.*, 2017, **117**, 1687–1764.
- 116 L. Xia, W. Fan, X.-A. Yuan and S. Yu, *ACS Catal.*, 2021, **11**, 9397–9406.